



**Universität für Bodenkultur Wien**  
University of Natural Resources  
and Life Sciences, Vienna

# Master Thesis

## **The role of RNA silencing factors in the control of virus invasion of the shoot apical meristem in *Arabidopsis thaliana***

submitted by

**Florian PRUCKNER, BSc**

in the framework of the Master program  
**Biotechnology**

in partial fulfilment of the requirements for the academic degree  
**Master of Science**

Vienna, January 22

Supervisor:

Univ.Prof.<sup>in</sup> Dr.<sup>in</sup> Margit Laimer

University of Natural Resources and Life Science

The work for this thesis was performed at the Gregor Mendel Institute of Molecular  
Plant Biology (GMI) at the Vienna BioCenter (VBC) and instructed by Univ. Doz.<sup>in</sup> Dr.<sup>in</sup>  
Ortrun Mittelsten Scheid and Dr. Marco Incarbone

## Affidavit

I hereby declare that I have authored this master thesis independently, and that I have not used any assistance other than that permitted. The work contained herein is my own except where explicitly stated otherwise. All ideas taken in wording or in basic content from unpublished sources or from published literature are duly identified and cited, and the precise references are included.

I further declare that this master thesis has not been submitted, in whole or in part, in the same or a similar form, to any other educational institution as part of the requirements for an academic degree.

I hereby confirm that I am familiar with the standards of Scientific Integrity and with the guidelines of Good Scientific Practice, and that this work fully complies with these standards and guidelines.

Vienna, 21 January 2022

Florian PRUCKNER (*manu propria*)

## Preface

This research was conducted at the Gregor Mendel Institute (GMI) in Vienna, a research institution of the Austrian Academy of Sciences at the Vienna BioCenter (VBC), between February 2021 and September 2021.

The research was funded by the GMI and the Lise-Meitner-Fellowship (M2921) from the Austrian Science Fund (FWF) to Marco Incarbone.

## Acknowledgements

I want to express my appreciation to all those who helped me in my project and who made it such a pleasant experience. I therefore want to thank the hosting research group being so welcoming from the start and enjoyable to work with until the very end. Especially I am thankful to my supervisor, Ortrun Mittelsten Scheid, who (in addition to supervising my scientific work) offered so much valuable support, advice, and guidance in career prospects and how to advance in the scientific world. I found myself quite inspired by her calm and well-organized leadership that seemed to push quite naturally everyone steadily into the right direction. Further I want to thank my mentor, Marco Incarbone, who provided me with the transgenic plants and viruses and instructed my experimental work. He was supporting me and the project continuously and readily throughout its course. With his patience, pleasant character and always open ears for ideas and discussion, I always felt encouraged, even if things did not go my way. Also, I want to highlight my appreciation to him and the PhD student Gabriele Bradamante, for the donation of uncountable bakery discount stickers. Finally, I want to thank the people of the VBC's Bio-Optics facility for their constant help on microscopy issues, the time they took for introductory courses and for providing me with the FIJI macro for image analysis that I used for this thesis. From BOKU University I especially want to thank Prof. Dr. Margit Laimer, for giving valuable advice on the writing of the thesis, and the interesting and pleasant discussions at several progress report presentations.

As a milestone in my education, I also want to thank my parents, Martina and Franz, for their personal and financial support over all these years. Further I want to thank my brother, Philip, for steadily providing me with inspiration and ambition by his deeply rooted determination and conviction to science. He was a role model for better time management and continuously inspired me to take opportunities. Last, but definitely not least, I want to give my special thanks to my good friend Martin Murauer, who – even though being in another field of science – provided me steadily with inspiration during several hours of discussion on science and more.

## Table of Content

Affidavit.....	2
Preface.....	3
Acknowledgements.....	4
Table of Content.....	5
Abstract.....	7
Kurzfassung.....	7
1) Introduction.....	9
1.1) RNA interference as virus defense in plants.....	9
1.2) Virus exclusion from the meristem.....	11
1.3) Role of RDR1 derived vasiRNAs upon virus infection.....	13
1.4) <i>Turnip mosaic virus</i> (TuMV).....	14
1.5) Meristem organization and cell fate of meristem layers.....	15
Meristematic organization via <i>WUSCHEL</i> and <i>CLV3</i> .....	15
Cell fate of the L1 and the L2.....	16
2) Aim of this Work.....	16
3) Methods and Materials.....	17
Plant material.....	17
Seed sterilization by chlorine gas.....	17
Growth Conditions.....	18
Virus material and preparation of inoculum solution.....	18
Infection experiments.....	18
DNA extraction.....	20
Protein extraction.....	20
RNA extraction.....	20
cDNA synthesis.....	21
PCRs.....	21
RT-qPCRs.....	22

Western Blots .....	22
4) Results .....	24
4.1) Role of RDR1 and RDR6 in virus exclusion of the shoot apical meristem .....	24
4.2) TuMV infection dynamics with daily resolution in Col-0 and <i>rdr1</i> (10-18 dpi) ....	30
4.3) Later TuMV infection dynamics in Col-0 and <i>rdr1</i> (17-23 dpi) .....	32
4.4) TuMV infection dynamics in Col-0 and <i>dcl2dcl3dcl4</i> .....	34
4.5) RDR1 is expressed in the stem parenchyma and leaf vasculature .....	36
4.6) Role of RDR1-produced vasiRNAs .....	39
5) Discussion .....	41
5.1) Possible explanations for TuMV meristem exclusion dynamics in <i>rdr1</i> plants ...	41
5.2) Virus load in Col-0 and <i>rdr1</i> plants .....	42
5.3) Lower virus concentration in the L2 of <i>rdr1</i> plants .....	43
5.4) <i>RDR6</i> and its role in virus meristem exclusion .....	43
5.5) Role of TuMV induced vasiRNAs and NBR1 in virus resistance .....	44
5.6) How does RDR1 mediate antiviral effects from a distance? .....	45
6) References .....	47
7) Annex .....	53
7.1) Solutions and buffers .....	53
7.2) List of Abbreviations .....	54

## Abstract

The ability of virus-infected plants to generate virus-free progeny was a crucial development in plant evolution. There is a lot of literature demonstrating that, in most plant/virus combinations, viruses are excluded from the shoot apical meristem (SAM). As the SAM is the center of apical organogenesis, and therefore gives rise to the reproductive organs and the germline, this phenomenon can inhibit vertical transmission of viruses to the next generation. Even though this exclusion is most likely a combination of several mechanisms, RNA interference (RNAi) has been identified as a major player in this phenomenon. Nonetheless, despite its undisputed importance, the exact silencing pathways and their regulation remain to a large extent unclear. Up to now, most studies have been performed in a rather static way, examining states of virus invasion and exclusion from the meristem at single timepoints. By observing virus infection around the SAM on a daily basis and by the use of a novel analysis technique to quantify the extent of invasion into the meristem, the more dynamic nature of this process could be captured. For *Turnip mosaic virus* (TuMV), a Potyvirus infecting *Arabidopsis thaliana*, it could be shown that prior to its exclusion from the meristem it accumulates therein. Furthermore, light is shed on the crucial role of the RNA-dependent RNA Polymerase 1 (RDR1) and its essential role as a silencing factor in this process. However, evidence presented in this work also suggests that RDR1 is not the only factor, but that there must be further mechanisms involved. This work further expands on where RDR1 is expressed, and how expression levels change upon TuMV infection. Finally, the potential roles of virus-activated small interfering RNAs (vasiRNAs) during infection are discussed.

## Kurzfassung

Die Fähigkeit von virus-infizierten Pflanzen, virus-freie Nachkommen zu produzieren, war eine maßgebende Entwicklung in deren Evolution. Umfassende Studien mit einer weiten Bandbreite an Pflanzen/Virus Kombinationen zeigen, dass in den meisten Fällen Viren daran gehindert werden, in das Sprossmeristem („shoot apical meristem“, SAM) einzudringen. Da das SAM der Ursprung der Reproduktionsorgane ist, stellt dieser Mechanismus eine essenzielle Barriere gegen die Weitergabe des Virus an die nächste Generation dar. Obwohl der genaue Mechanismus noch nicht aufgeklärt wurde und vermutlich aus einer Kombination verschiedener Elemente besteht, hat sich RNA Interferenz (RNAi) als wichtiges Prinzip darin herauskristallisiert. Nichtsdestotrotz

bleiben die Details dieses Verteidigungsprinzips in hohem Ausmaß unklar. Bis dato haben Studien zu diesem Phänomen versäumt, die Dynamik des Prozesses und dessen Zeitkomponente in Betracht zu ziehen. Mit einer neu entwickelten Analyse-methode konnte hier erstmals gezeigt werden, dass der Ausschluss von *Turnip Mosaic Virus* (TuMV) aus den SAM von *Arabidopsis thaliana* erst nach einer vorübergehenden Anreicherung im SAM stattfindet. Des Weiteren wird auf die Wichtigkeit der „RNA-dependent RNA Polymerase 1“ (RDR1) in diesem Vorgang eingegangen. Dennoch weisen die Ergebnisse, welche hier präsentiert werden darauf hin, dass auch noch weitere, RDR1-unabhängige Mechanismen am Werk sein müssen. Außerdem wird demonstriert, wie sich RDR1 Expression bei einer TuMV Infektion auf transkriptioneller Ebene sowie im Ort der Expression ändert. Abschließend wird darauf eingegangen welche Rolle RDR1 produzierte „virus-activated small interfering RNAs“ (vasiRNAs) haben könnten.

## 1) Introduction

Plant viruses are ever present in the natural flora. Today we know a broad spectrum of viruses that infect a wide array of plants. While some of these viruses seem latent and cause relatively weak or no symptoms, others can have devastating effects (Takahashi et al., 2019), especially in the monocultures of modern agriculture. To name just a few examples, *Tobacco mosaic virus* (TMV), *Cucumber mosaic virus* (CMV), *Cauliflower mosaic virus* (CaMV), and *Potato virus Y* (PVY) count among the most prominent plant viruses, with the highest economic impact (Scholthof et al., 2011). Hence, further understanding of how plants fight viral infections and how such knowledge can advance existing technologies to ensure reliable and efficient food production with the limited arable land at hand, will be of the utmost importance. Even though plants have a variety of defense mechanisms against viruses, one of the most effective and conserved is RNA interference (RNAi).

### 1.1) RNA interference as virus defense in plants

The general mechanism of RNA interference (RNAi) as a tool of defense and gene regulation is widely present among eukaryotes (Shabalina & Koonin, 2008) although there are some exceptions, like for example the model organism *Saccharomyces cerevisiae* (Drinnenberg et al., 2009). In plants, it is mainly implemented by three different classes of proteins: Dicer-like proteins (DCLs) that cut virus replication-derived double-stranded RNA into small fragments, RNA-dependent RNA polymerases (RDRs) that generate double-stranded RNA, and Argonaute proteins (AGOs) that associate with the small RNAs to target viral RNA. In the genome of *A. thaliana* there are four DCLs (DCL1 – DCL4), six RDRs (RDR1 - RDR6) and ten AGOs (AGO1 – AGO10). Generally, RNAi as a plant defense mechanism against viruses is triggered upon the presence of double-stranded RNA (dsRNA), either derived from replication intermediates or secondary structures of the RNA virus itself, or in case of DNA viruses, it can occur due to bidirectional transcription (Carbonell, 2017; Liu et al., 2009; Willmann et al., 2011).

dsRNA can be cleaved by DCL2 or DCL4 into 22 nt- or 21 nt-long virus-derived small interfering RNAs (vsiRNAs), respectively (Bond & Baulcombe, 2014). One strand of primary vsiRNAs can serve as primer for RDR1 or RDR6, that, with the help of antiviral RNAi-defective 1 (AVI1) and AVI2, synthesize the complementary RNA-strand of virus mRNAs (Guo et al., 2018). These dsRNAs again can be cleaved by DCL2 and DCL4

and hence, by production of secondary vsiRNAs, the number of small interfering RNAs (siRNAs) can be amplified. During RNA virus infection, the double-stranded secondary siRNAs can be loaded into AGO1, AGO2, and AGO5 and form the RNA-induced silencing complex (RISC) (Guo et al., 2018). Only the strand with the lower thermodynamic stability at its 5' end will stay associated with the AGO protein, while its complementary strand is lost and degraded (Schwarz et al., 2003). This mature antiviral RISC now can cleave homologous viral RNA in a sequence-specific manner (Guo et al., 2018), Fig. 1).

Plants lacking or having dysfunctional factors of the antiviral silencing pathway have been shown to be more susceptible to virus infection (Muhammad et al., 2019; Guo et al., 2018). For instance, knock-out mutants of *RDR1* show higher CMV RNA load and lower production of siRNAs against the virus. This is even more enhanced in the *rdr1rdr6* double mutant, whereas the *rdr6* single mutant does not deviate from the WT. Similarly, *dcl4* mutants accumulate much more virus RNA than the WT, further enhanced in the *dcl2dcl4* double mutant (Wang et al., 2010; Willmann et al., 2011).

Alongside the defense mechanisms of their host, viruses have evolved different ways to circumvent them. Nearly all plant-infecting viruses encode for proteins called viral suppressors of RNA silencing (VSRs) that hamper the host silencing mechanisms (Incarbone & Dunoyer, 2013). To name just a few examples: the 16K of *Tobacco rattle virus* (TRV), P1/HC-Pro of *Turnip mosaic virus* (TuMV), or 2b of *Cucumber mosaic virus* (CMV) (Fernández-Calvino et al., 2016; Kasschau et al., 2003; Lewsey et al., 2009).

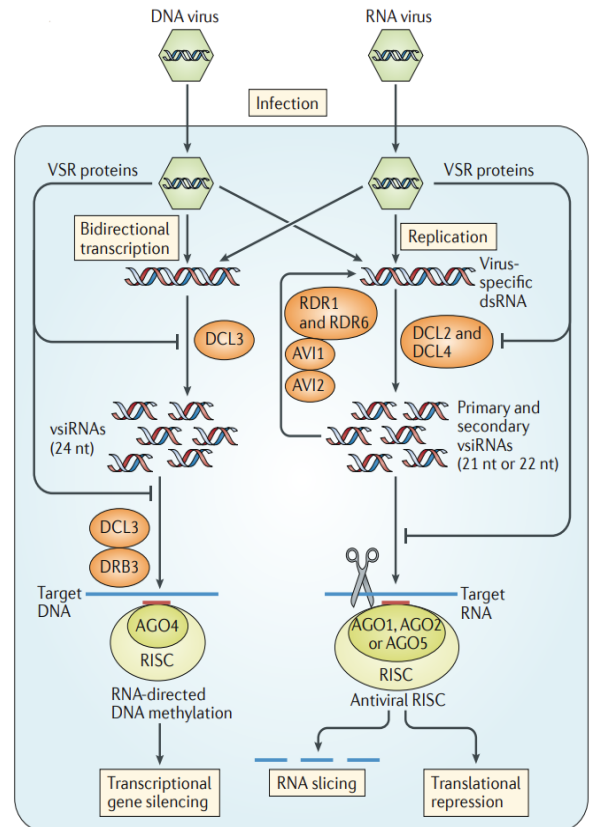


Fig. 1: **Antiviral RNAi in plants.** The process is triggered by the presence of double-stranded RNA in the cell. DCL2 and DCL4 cleave dsRNA and produce primary siRNAs. Possibly acting as primers, these enable the production of secondary vsiRNAs via RDR1 and RDR6. Primary and secondary vsiRNAs form a RISC with AGO proteins and guide the complex to its target site where it degrades viral RNA or inhibits translation. Cutting by DCL3 generates 24 nt vsiRNA, which can trigger transcriptional gene silencing via RNA-directed DNA methylation. Viruses can counteract silencing at several stages via viral suppressors of RNA-silencing (VSRs) (Guo et al., 2018).

## 1.2) Virus exclusion from the meristem

Despite systemic virus replication and spread throughout whole plants, the exclusion of viruses from the reproductive organs and their origin, the SAM, is a commonly observed phenomenon in many virus/host combinations (reviewed in Bradamante et al., 2021). Exclusion from the SAM has been suggested to limit vertical transmission of viruses to the progeny (Johansen et al., 1994). However, the molecular mechanisms behind this phenomenon remain to be determined to a great extent. Either the movement into and/or the replication of the virus in the meristem could be inhibited, and in two different ways. (1) The defense could be always active, excluding viruses constitutively. (2) The defense mechanism could be only activated once a plant is infected with a virus (Bradamante et al., 2021). Concerning the second possibility, the questions are how, when, and where the plant can sense the virus and activate the corresponding pathways that protect the meristem from invasion. It could be that the meristem is primed against the entrance of a virus before its arrival, via signaling factors that move ahead of the virus invasion front. These could be hormones, like salicylic or abscisic acid that already have been linked to viral defense and activation of silencing factors (Alazem et al., 2019). On the other hand, it could be mediated via siRNAs and silencing factors that move into the meristem themselves, thereby activating the defense mechanisms that effectively exclude the virus from this organ later.

A handful of RNA silencing components have been shown to play a significant role in virus exclusion from meristems. *NbRDR6* in *N. benthamiana* is required for the exclusion of *Potato virus X* (PVX) and *Potato spindle tuber viroid* (PSTVd) (Schwach et al., 2005; Di Serio et al., 2010). There is some published evidence that also *RDR1* could have an important role, as transgenic overexpression of *MtRDR1* of *Medicago truncatula* in *N. benthamiana* resulted in TMV being impaired in movement toward the growth apices (Lee et al., 2016). The role of Dicer-like proteins (DCLs) needs still to be investigated. One study however showed that knocking down *NbDCL2* and *NbDCL4* expression in *N. benthamiana* did not result in meristem invasion by *Cymbidium ringspot virus* (CymRSV) lacking its P19 VSR. However, as *DCL2* and *DCL4* expression levels were not evaluated, it is not clear if their function was indeed extinguished. There are no studies yet investigating the role of AGOs in the exclusion of virus from the meristem. WUSCHEL (WUS) is a transcriptional factor, expressed in the meristem, that is essential for its size regulation and structural organization. It has been shown that upon overexpression of WUS, the accumulation of *Cucumber mosaic virus* genomic RNA was inhibited in the

meristem (Wu et al., 2020). The fact that the pattern and extent of meristem infection varies greatly between different plant-virus combinations reflects the complexity of this phenomenon.

To establish antiviral silencing in a virus-free SAM, it is suggested that vsiRNAs of infected cells move into the SAM and surrounding tissue either with the virus or prior to the infection front (Charles et al., 2011). However, evidence that vsiRNAs can enter the SAM and establish silencing of transgenes is conflicting. It was shown that PVX in *N. benthamiana* caused systemic virus-induced gene silencing (VIGS) except in the SAM (Ruiz et al., 1998). Also, in *N. benthamiana* the introduction of ectopic DNA induced systematic silencing that spread throughout the plant, but not into the shoot apices (Voinnet et al., 1998). These studies therefore suggest that vsiRNAs cannot trigger silencing in the meristem. On the other hand, contradicting evidence shows that *Pea seed-borne mosaic virus* (PSbMV), even though unable to enter the SAM, could silence a systematically expressed transgene in the SAM (Jones et al., 1998). Furthermore, the meristem-excluded *Tomato golden mosaic virus* (TGMV) carrying a homologous sequence of a meristematic gene, was able to silence that gene in *N. benthamiana* plants (Peele et al., 2001). The role of RNAi in exclusion of virus from the meristem therefore remains largely unclear.

Alternatively to RNAi as a mechanism of action, there is also evidence that the regulation of plasmodesmata size could play a vital role. Two proteins of the gene family *Plasmodesmata Located Protein 1* (*PDLP1*) have been identified to be expressed in the shoot apex (Bayer et al., 2008). Some viruses express movement proteins that can interact with proteins of the PDLP1 family and form tubular structures in the plasmodesmata that can enhance virus and virion movement (Amari et al., 2010). The size of plasmodesmata is also proposed to be regulated by viruses through induction of callose-degrading glucanase activity (Zavaliev et al., 2010).

Generally, intracellular virus movement is dependent on microfilaments (Pitzalis & Heinlein, 2018). As microfilament depolymerization is essential for *de novo* meristem formation (shown in callus cultures) (Tang et al., 2017), it would be informative to illustrate the state of microfilament polymerization *in vivo* in SAMs. It could be that restricted virus movement is also connected with a depolymerized state of microfilaments, limiting the movement of virus in those compartments to diffusion only and making it unlikely that they would find their way to the intracellular location of replication, as well as their progression afterwards to the periphery of the cell.

Additionally, there are possibly also other mechanisms, and it is likely that virus control in the meristem is due to a mixed combination of the mechanisms mentioned above, and yet others to be discovered.

### 1.3) Role of RDR1 derived vasiRNAs upon virus infection

One function of RDR1 is the production of virus-activated small interfering RNAs (vasiRNAs) during virus infection (Cao et al., 2014). These siRNAs derive from endogenous genes and their functions are still a subject of investigation. However, in *A. thaliana*, vasiRNAs can target and down-regulate endogenous transcripts during infection with CMV deficient in its 2b VSR (CMV-Δ2b) (Cao et al., 2014). 2b is sufficient to block vasiRNA biosynthesis in case of CMV infection, whereas vasiRNA production was maintained to some extent upon TuMV infection. Via degradome and sRNA sequencing, it has been demonstrated that vasiRNAs can indeed target endogenous transcripts for sequence-specific cleavage during TuMV infection in oilseed rape (Pitzalis et al., 2020). Interestingly, in this study, they also observed trans-acting vasiRNAs that targeted other endogenous transcripts than the ones they are derived from.

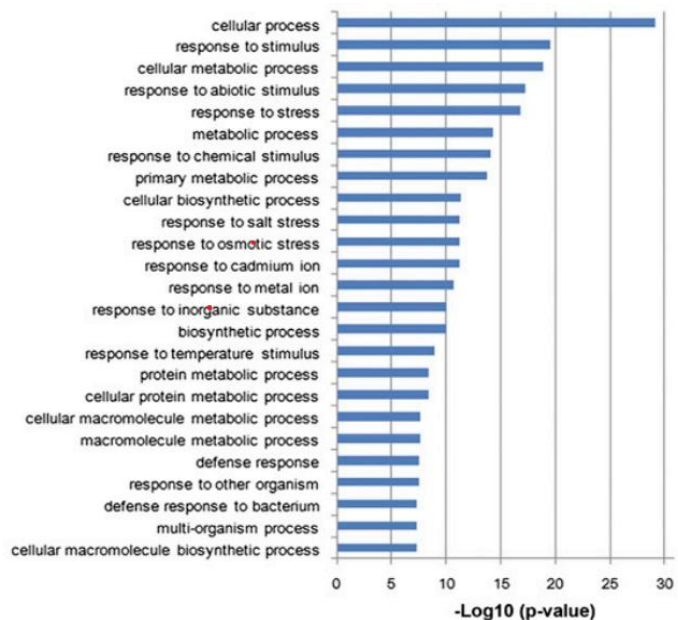


Fig. 2: **25 most prominent gene functions linked to vasiRNA targets in CMV-Δ2b and TuMV-GFP infected *A. thaliana* plants.** Data was obtained via gene ontology analysis (Cao, et al., 2014)

Gene ontology analysis revealed that genes targeted by vasiRNAs upon TuMV and CMV infection are mostly linked to responses to chemical, biotic, and abiotic stimuli, stress, interactions with other organisms, and general defense responses (Cao et al., 2014; Fig. 2). While more detailed research is needed, this could indicate that either vasiRNAs are advantageous to the virus and suppress the host's lines of general defense, or that vasiRNAs are used by the host to modulate the expression of specific defense genes.

#### 1.4) Turnip mosaic virus (TuMV)

TuMV is a plant virus species of the family *Potyviridae*, causing diseases in cruciferous plants. It is usually transmitted via different aphid species. Infected plants show symptoms like chlorotic local lesions, mottling, puckering, and distortions. TuMV consists of an approximately 10 kb-long, positive polarity single-stranded RNA genome with a filamentous capsid formed by helical arrangement of coat protein units. The genes of TuMV are encoded as a polyprotein (Fig. 3). The rod-like virus is flexible and can vary in length (Cuesta et al., 2019). TuMV replicates in ER-derived virus-induced vesicles, also called virus replication factories. These structures are vesicles that vary in size from 0.6 to 4.3  $\mu\text{m}$  and move in a unidirectional manner from the ER to the periphery of the cell. Due to the high viscosity of the cytoplasm, bigger vesicles require active transport along the microfilaments (Grangeon et al., 2010).

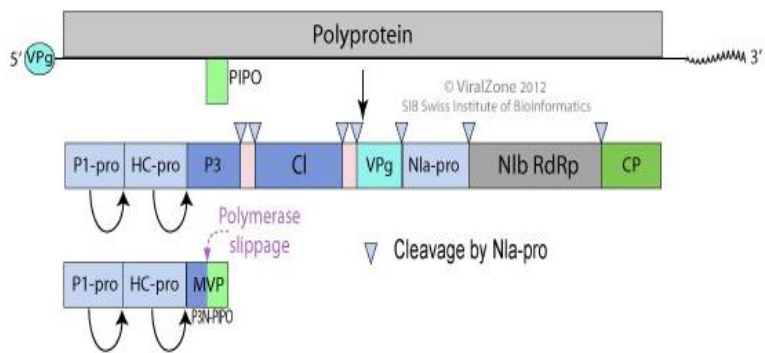


Fig. 3: **Genome organization of potyviruses** (Viralzone, 2012)

VPg, a uridylylated protein, can bind the 5'-end of TuMV's genomic RNA and serve there as a nucleotide-peptide primer. TuMV encodes for two polyproteins, which are further cleaved by its proteases Nla-pro, P1, and HC-Pro into at least ten individual proteins (UniProt, 2021). The P3N-PIPO polyprotein is cleaved by P1 and HC-Pro proteinases, thereby resulting in the production of three individual proteins. The P1 proteinase and the HC-Pro cleave only at their own C-termini (UniProt, 2021).

Besides its function as a protease, HC-Pro acts also as a VSR in several different ways. Several studies of different potyviruses have shown the ability of HC-Pro to interfere with a variety of steps in the virus silencing pathway. These include the inhibition of vsRNA uploading by their sequestering, interference with vsRNA methylation by inhibiting cofactor production, binding and inactivating the methyltransferase HEN1, and downregulation of *AGO1* and *RDR6* (Valli et al., 2018). Importantly, binding and sequestration of 21-22 nt-long siRNA has been shown to be necessary for TuMV to establish systemic infection in *A. thaliana* (Garcia-Ruiz et al., 2010). A further mode of action could be the mis-regulation of sRNA production, as HC-Pro has been shown to upregulate *FIERY 1 (AtFRY1)* (Endres et al., 2010), which was shown to increase the

miRNA/siRNA ratio that is loaded onto AGO1 (You et al., 2019). There is also evidence that HC-Pro can dampen the salicylic acid response after a virus infection by interaction with AtCA1, an activator of the salicylic acid pathway and inducer of SA accumulation (Poque et al., 2017). As a defense mechanism against this potent VSR, the selective autophagy cargo receptor AtNBR1 of *A. thaliana* can bind HC-Pro and thereby suppress TuMV infection by limiting the viral silencing suppressing effects (Hafrén et al., 2018). The wide variety of mechanisms of action of HC-Pro as a VSR highlights the complexity of the interplay between viruses and plants and suggest that further functions of HC-Pro may yet to be discovered.

## 1.5) Meristem organization and cell fate of meristem layers

### Meristematic organization via *WUSCHEL* and *CLV3*

To remain in proper size, the organization of the meristem is based on a negative feedback loop between the stem cells and the so-called organizing center (OC). The stem cells are located in the middle of the meristem on the three most peripheral cell layers. These layers, in respect to their location from top to bottom are called L1 (outermost layer), L2 (second layer), and L3 (innermost layer). In basal proximity of the L3 lays the OC. The OC contains about ten cells, that, under control of the transcription factor *WUSCHEL* (*WUS*), produce a still unknown signaling factor that induces expression of *CLAVATA3* (*CLV3*) in the stem cells (Dodsworth, 2009). This small peptide is secreted and diffuses to the OC.

There it can bind the dimeric receptor containing *CLV1* and *CLV2*, which results in the downregulation of *WUS* expression (Müller, 2007; Fletscher, 2018). The location of the stem cells and the organizational center and the scheme of their interactions can be seen in Fig. 4. The meristematic stem cells are organized into two layers (L1 and L2) at the periphery that form due to their anticlinal cell division pattern, and the corpus (L3) that is in the center. These layers all give rise to distinct tissue types (Malhan et al., 2015).

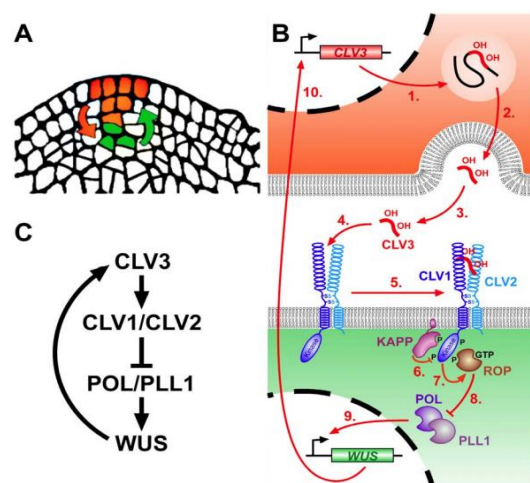


Fig. 4: **Scheme of meristem organization by *WUS-CLV3* negative feedback loop.** A: Location of stem cells (orange) and organizing center (green). B: Signaling pathway between *CLV3* and *WUS*. C: Summary of the negative feedback loop (Müller, 2007).

## Cell fate of the L1 and the L2

Stem cells of the L1 have been shown to be the source of most of the epidermal cells in organs like receptacle, petals, anthers, filaments, style, stigma, and the ovule (Shu et al., 2012; Hernandez-Lagana et al., 2021). Crossing experiments with periclinal chimeras, carrying a different allele in the L1, demonstrated that no progeny inherited an L1 marker gene. Cells of L2 origin were shown to give rise to the outer mesophyll as well as outermost cortical parenchyma and notably, gametes. L3 cells give rise to inner cortex, vascular tissues, roots, and pith (Shu et al., 2012).

## 2) Aim of this Work

The aim of this work was to gain novel insights, on how viruses are excluded from the SAM. In particular, interest lay on answering the question if virus exclusion from the meristem needs a prior phase of virus accumulation therein to trigger a reaction, or whether it occurs constitutively. Therefore, it was necessary to characterize this phenomenon over a given time period, to be able to grasp any dynamic effects. As virus accumulation in and around the meristem, to the best of our knowledge, never has been quantified, particular interest further lay in the development of a method capable to do so. It should be shown that the method would be able to consistently deliver reproducible results in different experiments. In the best case, the developed method would be able to serve as a novel tool in the field of science investigating the meristem exclusion of viruses.

Using this method, the effect of different knock-out mutations in the RNA silencing pathway on virus exclusion from the meristem should be demonstrated. Starting point for these experiments should be the analysis of wild-type *A. thaliana* plants and the *rdr1* and *rdr6* mutants.

This work not only should extend our knowledge on this phenomenon but should also serve as a proof of concept on how virus meristem invasion/exclusion could be quantified.

### 3) Methods and Materials

The composition of different solutions and buffers can be found in the annex.

#### Plant material

For all experiments *Arabidopsis thaliana* plants of the ecotype Columbia (Col-0), and derived mutants from this line were used. Meristem-specific reporter lines were generated by ectopically expressing a H2B histone tagged with green fluorescent protein (Clover) under the meristem-specific CLAVATA 3 (CLV3) promoter. The Col-0/pCLV3::H2B-Clover line was previously generated in the lab and crossed with *rdr1-1rdr6-15* (Garcia-Ruiz et al., 2010) and *dcl2-1dcl3-1dcl4-2* (Deleris et al., 2006) to obtain the mutant combinations described, expressing the fluorescent marker in the meristem (Tab.1). The resultant lines were verified to be homozygous for T-DNA insertions by PCR genotyping and for transgene locus through selection on hygromycin. Analogously RDR1-reporter lines Col-0/pRDR1::H2B-Clover lines and were also previously generated in the lab.

Mutant	Transgene
Col-0 (WT)	/
Col-0	pCLV3::H2B-Clover
<i>rdr1</i>	pCLV3::H2B-Clover
<i>rdr6</i>	pCLV3::H2B-Clover
<i>rdr1rdr6</i>	pCLV3::H2B-Clover
<i>dcl2dcl3dcl4</i>	pCLV3::H2B-Clover
Col-0	pRDR1::H2B-Clover

Tab.1: **Genotypes of all *A. thaliana* lines used in this thesis.**

#### Seed sterilization by chlorine gas

Seeds were incubated at -20 °C O/N and sterilized the next day by chlorine gas sterilization at room temperature. The whole procedure was performed under the fume hood. The seeds were placed into a plastic box (approximately 40x25x15cm) in open 1,5 ml microcentrifuge tubes. An open plastic cup, containing approximately 100ml of bleach was also placed in the box. Approximately 15 ml of hydrochloric acid were added to the bleach, to produce chlorine gas. The container was closed quickly. After approximately 15 minutes the container was opened again to let the gas dissipate.

## Growth Conditions

All plants were sown and grown in 12h/12h light/dark days under LED lighting (with a photosynthetically active photon flux density (PPFD) of 122,4  $\mu\text{mol}/\text{m}^2\text{s}$  [PPF-Blue / Green / Red = 26,0 / 37,4 / 59,0  $\mu\text{mol}/\text{m}^2\text{s}$  respectively]). After approximately 4 weeks after sowing, before bolting, the plants were infected and transferred to another chamber reserved for viral infections with 16h/8h light/dark days with the same settings for PPFD.

## Virus material and preparation of inoculum solution

Leaves of *Nicotiana benthamiana* plants systemically infected with *Turnip mosaic virus* (UK1 isolate) were used for inoculum preparation. The virus clone encoding for an additional 6K2 protein, fused with a red fluorescent protein (scarlet) (TuMV-6K2:Scarlet) was previously generated in the lab, stored at -80 °C and delivered through *Agrobacterium tumefaciens* inoculation. At all working steps the material remained frozen by keeping it in liquid nitrogen. A mortar was pre-cooled with liquid nitrogen. Approximately 100 mg of frozen tissue was added for each 2 ml of prepared inoculum solution. Approximately 15 ml of liquid nitrogen was added to the tissue in the mortar, and it was ground with a pestle until pulverized. This was repeated a second time. 2 ml of virus inoculation buffer for each 100 mg of ground leaf tissue was added, and the mix was further homogenized with the pestle. The solution was transferred into 2 ml microcentrifuge aliquots and always kept on ice. The aliquots were turned at 20 rpm on a wheel for 10 min at 4 °C. Next the aliquots were centrifuged at 2000 rpm for 2 min at 4 °C. The supernatant was transferred into fresh tubes. The fresh infection mix was always kept on ice and was used immediately after preparation.

## Infection experiments

### *Infection by mechanical inoculation*

Prior to mechanical inoculation the plant leaves were sprinkled with Celite® crystalline abrasive powder. A cotton swab was dipped into the inoculum solution and gently rubbed over four to five leaves per plant, two to three times per leaf. The Celite® powder caused small disruptions in the leaf surface to enable virus infection. After mechanical inoculation, the plants were sprayed shortly with water to remove excessive amounts of Celite® powder, that could otherwise cause further stress to plants. For mock infections, plants were treated in the same way, but rubbed with inoculation buffer only.

#### *Harvesting of meristems and dissection*

Apical parts of the plant shoot, containing the SAM, were picked off by hand and stored in 50 ml centrifugation tubes that contained a wet piece of paper to ensure high air moisture and to extend the time shoots stayed fresh and would not wilt. Under a stereomicroscope the excessive flowers and flower buds were picked off with pointy tweezers to ensure a clear observation of the SAM later. Only smaller developing flower buds close to the meristem were left. Approximately 2 mm of the most apical part of the shoot were picked off and stored in microcentrifuge tubes, containing 300  $\mu$ l of fixing solution. The microcentrifuge tubes were placed with open lids in a vacuum chamber for 10 minutes, to ensure infiltration of the fixing solution throughout the tissue. Next the tubes were incubated at 37 °C for 40 min to allow the formaldehyde to fix the tissue. The dissected meristems were stored in 700  $\mu$ l of MTSB at 4 °C.

#### *Clearing of tissue and preparation of microscopy slides*

The reagent ClearSee™ was used to clear the tissue. For this the MTSB buffer, used for the storage of the tissue, was replaced with 500  $\mu$ l of ClearSee™ solution containing DAPI and was incubated for at least two days at 4 °C.

Next, the meristems were placed on microscopy slides and embedded in ClearSee™ solution. To ensure that meristems were not squeezed or crushed too much, small droplets of Vaseline® were placed on the slide, where the corners of the cover slide were then placed, to form spacers. After about 45 min the cover slide was sealed off with nail polish. The samples were imaged on the same day.

#### *Microscopy and acquisition parameters*

In time-course experiments, all acquisitions were performed with a confocal point scanning microscope (LSM 710 2Pi Axio Observer (inverted)) with an 25x immersion objective, that was adjusted to the refractive index (RI) of an immersion medium. As an immersion medium a glycerin-water mixture with a RI of 1,42 was used (the same as the RI of ClearSee™). As an interface for image acquisition the ZEN® software was used. Acquisition parameters were not changed throughout individual experiments. In case of oversaturation, all laser intensities were put to 50% of prior acquisitions, to ensure further proportionality between different fluorescence intensities. In the transcriptional reporter experiment (Fig. 17 & 19) a 10x objective was used.

#### *Image analysis*

Via a FIJI macro the fluorescence (provided by Thomas Lendl at the Bioptics facility)

relative intensities were integrated over a drawn line with a defined width of 100 (Fig. 6). The values were stored, processed, and analyzed in excel, to create the plots.

For graphical description of the overall workflow of infection experiments and their analysis see also Fig. 5.

#### DNA extraction

200  $\mu$ l of DNA extraction buffer were put into a tube with 5-7 glass beads. The tissue of interest was added, and the samples were disrupted by shaking at  $30 \text{ s}^{-1}$  for 2 min. The mix was incubated on a heating block at  $95 \text{ }^{\circ}\text{C}$  at 1300 rpm for 10 min. The mix was centrifuged at 6000 rcf for 10 s and the supernatant transferred to a new tube. This process was repeated. The DNA extract was stored in a new tube at  $-20^{\circ}\text{C}$ . Cotyledon tissue was used for genotyping.

#### Protein extraction

Approximately 100 mg of plant tissue were harvested and frozen in liquid nitrogen. The tissue was disrupted with glass-beads by shaking at  $30 \text{ s}^{-1}$  for 1 min. 300  $\mu$ l of Laemmli buffer was added and vortexed until the liquid thawed. The liquid was shortly spun down in a centrifuge. The tubes were shaken on heating block at  $95 \text{ }^{\circ}\text{C}$  at 500 rpm for 10 min. Afterwards they were shaken on heating block for 30 min. at room temperature at 500 rpm. The samples were centrifuged at 13000 rpm speed for 45 min and the supernatant was transferred to a new tube and stored at  $-20 \text{ }^{\circ}\text{C}$ .

#### RNA extraction

Tubes with 6-9 glass-beads were prepared. 4-6 young inflorescences were added to each tube and immediately put to liquid nitrogen. Disruptor barrels were pre-cooled at  $-80 \text{ }^{\circ}\text{C}$ . Tissue was disrupted by shaking at maximum amplitude at shaker for 1 min. Immediately 1 ml of TRIZOL was added to the tissue. The tubes were vortexed and incubated at room temperature for 10 min. The samples were centrifuged at 12000 rcf for 10 min. at  $4 \text{ }^{\circ}\text{C}$  and the supernatant was transferred to new tubes. 0,2 ml of chloroform was added to the tubes these were vortexed vigorously for 15 s. The samples were incubated at room temperature for 3 min. After centrifugation at 12000 rcf for 1 min. at  $4 \text{ }^{\circ}\text{C}$ , the aqueous upper phase was transferred to a new tube (ca. 50-60 % of TRIZOL

volume). RNA was precipitated by mixing with 1 volume of isopropanol and incubation for at least 30 min. on ice. Samples were centrifuged at 12000 rcf for 15 min. at 4 °C to obtain pellets. The supernatant was removed, and pellets washed with 350 µl of 80% ethanol. After short vortex the samples were centrifuged at 12000 rcf for 5 min. at 4 °C. Ethanol was removed and the pellets were dried at room temperature. Pellets were dissolved in RNase-free water by incubating at 60 °C for 10 min. Samples were quantified with a nanodrop (Thermo Fisher Scientific) and stored at -20 °C.

### cDNA synthesis

RNA samples were treated with DNase (Thermo Fischer Scientific), according to manufacturer's instructions. cDNA was generated with the RevertAid H Minus First Strand cDNA Synthesis Kit© of Thermo Fisher® according to manufacturer's instructions, from 500 ng of DNase-treated RNA per sample, and using an oligo-dT primer. cDNA was stored at -20 °C.

### PCRs

All non-quantitative PCRs were performed as followed:

Mix:

Taq-Polymerase	1 µl
Taq-Pol. Buffer (2x)	10 µl
FW-Primer (1:10)	1 µl
RV-Primer (1:10)	1 µl
DNA	1 µl
ddH <sub>2</sub> O	ad. 20 µl

Thermocycler Setting:

95 °C	300s	35x
95 °C	30s	
60 °C	60s/kb	
72 °C	30s	
72 °C	300s	
10 °C	600s	

## RT-qPCRs

All quantitative real-time PCRs were performed using the FastStart Essential DNA Green Master<sup>®</sup> Kit and the Lightcycler<sup>®</sup>96 instrument and software as described in the associated protocol.

Thermocycler Setting:

95 °C	600s
95 °C	10s
60 °C	40s
97 °C	1s

↻ 45x

## Western Blots

### *Protein separation per SDS-PAGE*

	Resolving Gel (15%)	Stacking Gel (4%)
Acryl/Bis 37,5:1	7,5 ml	1,5 ml
Buffer*	6,6 ml	2,8 ml
H <sub>2</sub> O	5,7 ml	10 ml
APS 10%	200 µl	150 µl
Temed	20 µl	16 µl

**\*Stacking Buffer:**

Tris	37,8g
pH	=6,8
SDS 20%	12,5 ml
H <sub>2</sub> O	ad. 500 ml

**\*Resolving Buffer:**

Tris	68g
pH	=8,8
SDS 20%	7,5 ml
H <sub>2</sub> O	ad. 500ml

**Running Buffer:**

Tris-Glycine Buffer	1x
SDS	0,1%

Gel was run at 80V with proteins in stacking gel and with 100V when they reached the resolving gel.

### *Transfer*

Membrane was incubated in 80% ethanol for 5min. A Western Blot sandwich was made, and the proteins were transferred to the membrane for 1,5h at 80V.

Transfer Buffer:      Tris-Glycine 1x  
                                 Ethanol 20%

### *Membrane blocking and incubation with primary and secondary antibody*

The membrane was washed for 5 min. in PBS 1x, Tween 0,1%. Next the membrane was saturated by incubating it for 30 min. in PBS 1x, Tween 0,1%, milk powder 5%. The membrane was incubated ON in PBS 1x, Tween 0,1%, milk powder 5%, primary antibody 1:1000 (NBR1-antibody, AS14 2805, Agrisera). Afterwards it was washed 4 times for 10 min with PBS 1x, Tween 0,1%. The membrane was saturated by incubation for 30 min. in PBS 1x, Tween 0,1%, milk powder 5%. It was incubated for 2h in PBS 1x, Tween 0,1%, milk powder 5%, secondary antibody (anti-mouse coupled with HRP) 1:1000. Afterwards it was washed 4 times in PBS 1x, Tween 0,1%.

### *Acquisition and analysis*

For visualization the SuperSignal™ West Pico PLUS Chemiluminescent Substrate from Thermo Scientific was used, following the protocol. Acquisitions were taken with the iBright 1500 machine from Invitrogen by Thermo Fisher.

## 4) Results

### 4.1) Role of RDR1 and RDR6 in virus exclusion of the shoot apical meristem

Most potyviruses are thought to be unable to enter the meristem, except for some that are known to be seed-transmissible (López-Moya & García, 2008). *Turnip mosaic virus* (TuMV) was chosen for the experiments presented here, as it easily establishes systemic infection in *A. thaliana*. Stable clones expressing fluorescent proteins have already been used numerous times, and a body of evidence exists on how TuMV interfaces with host RNAi (Vijayapalani et al., 2012; Li et al., 2016; Garcia-Ruiz et al., 2010). The use of a recombinant virus expressing a fluorescent protein allows the preparation and observation of a large number of meristems with relative ease, as opposed to detection of virus through *in situ* hybridization, which is a standard in the field but comparatively complex and labor-intensive. To determine whether TuMV is excluded from the shoot apical meristem (SAM) upon infection of *A. thaliana*, a time-course experiment was performed, evaluating the virus progression at four different days post infection (dpi). Previous experiments in the lab had shown that TuMV can invade the meristem in *rdr1* mutants of *A. thaliana*, and data from the literature indicated that *RDR6* is able to exclude viruses and viroids from *N. benthamiana* SAM (Di Serio et al., 2010, Schwach et al., 2005). Therefore, we wondered whether and how the infection dynamics would differ between Col-0 (wild type) and the *rdr1*, *rdr6*, and *rdr1rdr6* double knock-out mutants. To visualize the SAM, plants ectopically expressing a H2B histone tagged with green fluorescent protein (Clover) under the meristem-specific CLAVATA 3 (CLV3) promoter (pCLV3::H2B-Clover) were used. To visualize TuMV, plants were infected with a virus variant generated in the lab, expressing a red fluorescently tagged version of its 6K2 protein (TuMV-6K2:Scarlet), which associates with virus replication complexes (Jiang et al., 2015). The plants were mechanically infected shortly before starting to bolt. 7-12 SAMs of different TuMV- and mock-infected plants of each genotype were dissected at 9, 11, 13, and 15 dpi. The tissue was fixed and cleared, then close-up images of the green fluorescently tagged meristems were acquired with a point-scanning laser confocal microscope.

Once all images were acquired, the workflow proceeded as summarized in Figure 5. Using an image analysis macro in FIJI, a line with a defined width was drawn vertically along the center of each meristem and the fluorescence level was quantified in the area

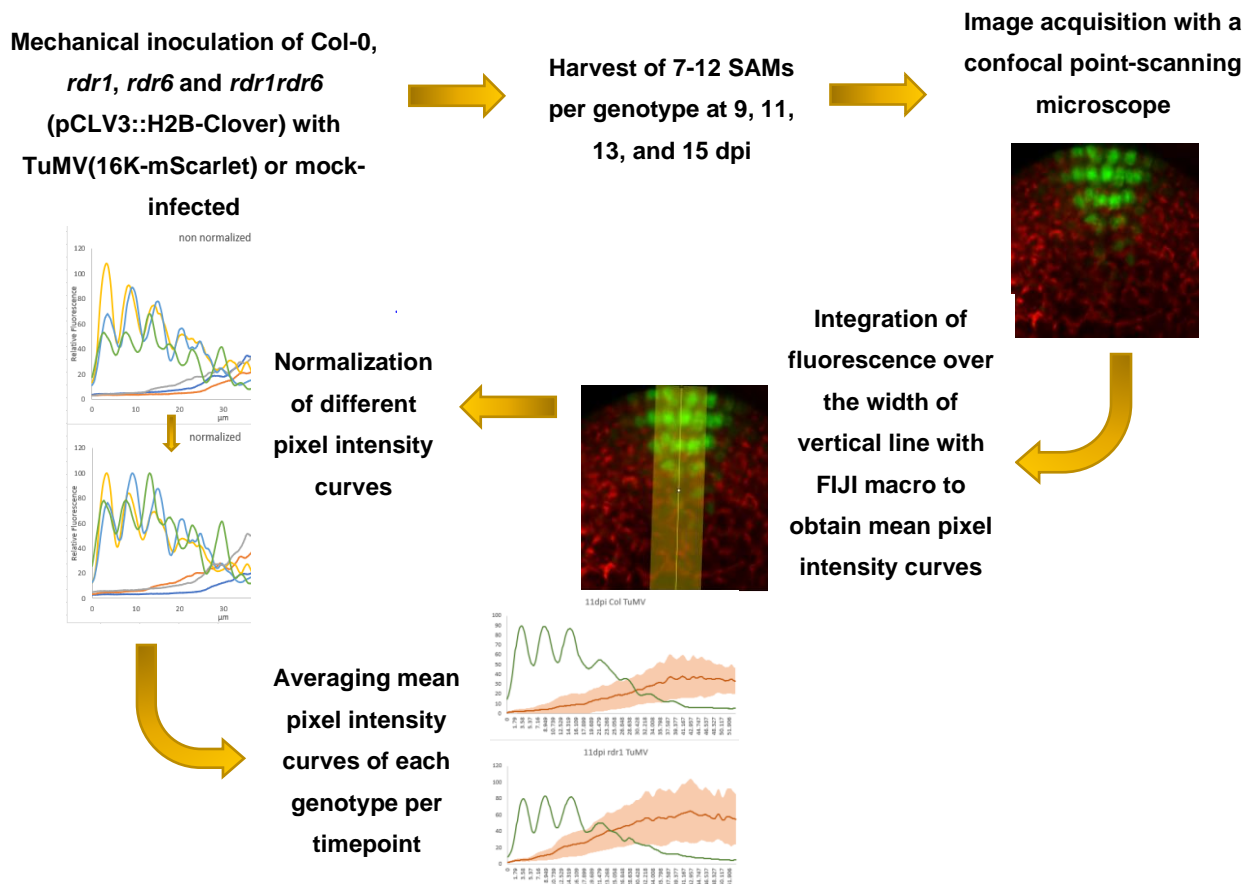


Fig. 5: **Workflow of the time-course experiment.** (1) Mechanical inoculation of plants, (2) Harvest of meristems at different days after infection, (3) Image acquisition under a point scanning confocal microscope, (4) Measurement of green and red fluorescence intensities over a vertical line with defined width, (5) Normalization of fluorescence intensities, (6) Averaging of all fluorescence intensities for each genotype and timepoint.

covered by the width of the line (Fig. 6). This macro integrated the fluorescence intensity separately for each wavelength. Therefore, the macro could be used to quantify the progression of the red-fluorescent virus proteins into the green-fluorescent meristematic stem cells. Acquisition parameters of the confocal microscope were kept constant throughout the experiment and thereby allowed comparing fluorescence levels of different samples. The intensities of meristematic green fluorescence varied considerably. This could be due to flower primordia covering the meristems, or to different depths at which the meristems were embedded in the mounting medium. As fluorescence emission intensities are directly proportional to their excitation intensities, the mean green fluorescence curves of all meristems could be normalized to have a maximum green fluorescence level of 100, with the red fluorescence levels being adjusted with the same normalization factor. After normalizing, mean pixel intensity curves of all plants of each timepoint and genotype were averaged, to obtain a

representative graph, summarizing the state of virus infection for each genotype per timepoint (Figure 5, bottom). To control the deviation of virus accumulation and progression in these graphs, also the area of one degree of standard deviation was plotted around the averaged mean red pixel intensity curve.

The meristems analyzed per timepoint vary because some meristems did not show any red fluorescence (even in the stem) and were considered as deriving from non-systemically infected plants and discarded. Some were damaged during dissection or disrupted in other ways during handling and did not provide useful images. The infection worked well, with approximately 80-90% of inoculated plants showing systemic symptoms such as curled and distorted leaves and shoots. The fastest traveling part of the virus infection front was mainly located in the middle of the stem, close to the vasculature. With the graphs derived from the FIJI macro fluorescence analysis of a mock-infected plant, it was possible to differentiate the different cell layers – the L1, L2 and L3 – of the meristem (Fig. 6).

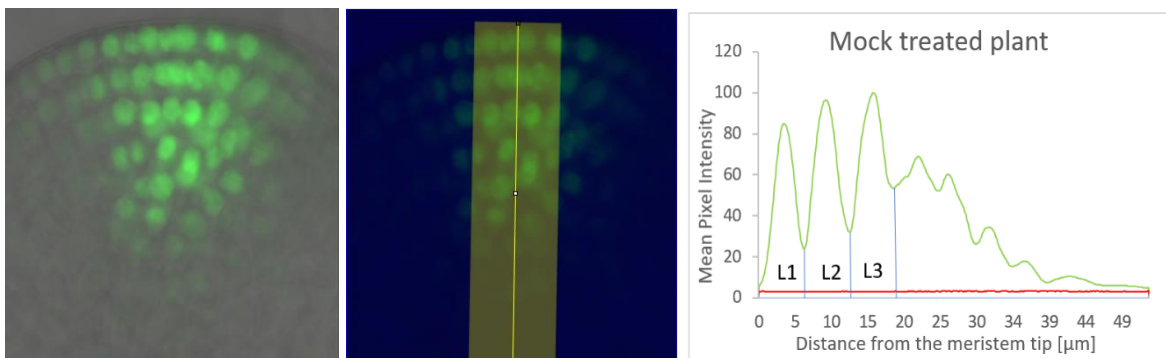


Fig. 6: **Image processing of a meristem of a mock-treated plant.** Left: Acquisition from the confocal microscope. Middle: In the FIJI Macro, the fluorescence over the vertical line is integrated. Right: Mean pixel intensities are plotted in a diagram. No red fluorescence can be seen, as the plant was mock-treated.

Red fluorescent TuMV was observed in all genotypes and at all timepoints (Fig. 7). The graphs in Fig. 8 summarize the progression of the TuMV infection in each genotype at each observed timepoint. The number of meristems used for the averaged graphs is indicated in each graph with N.

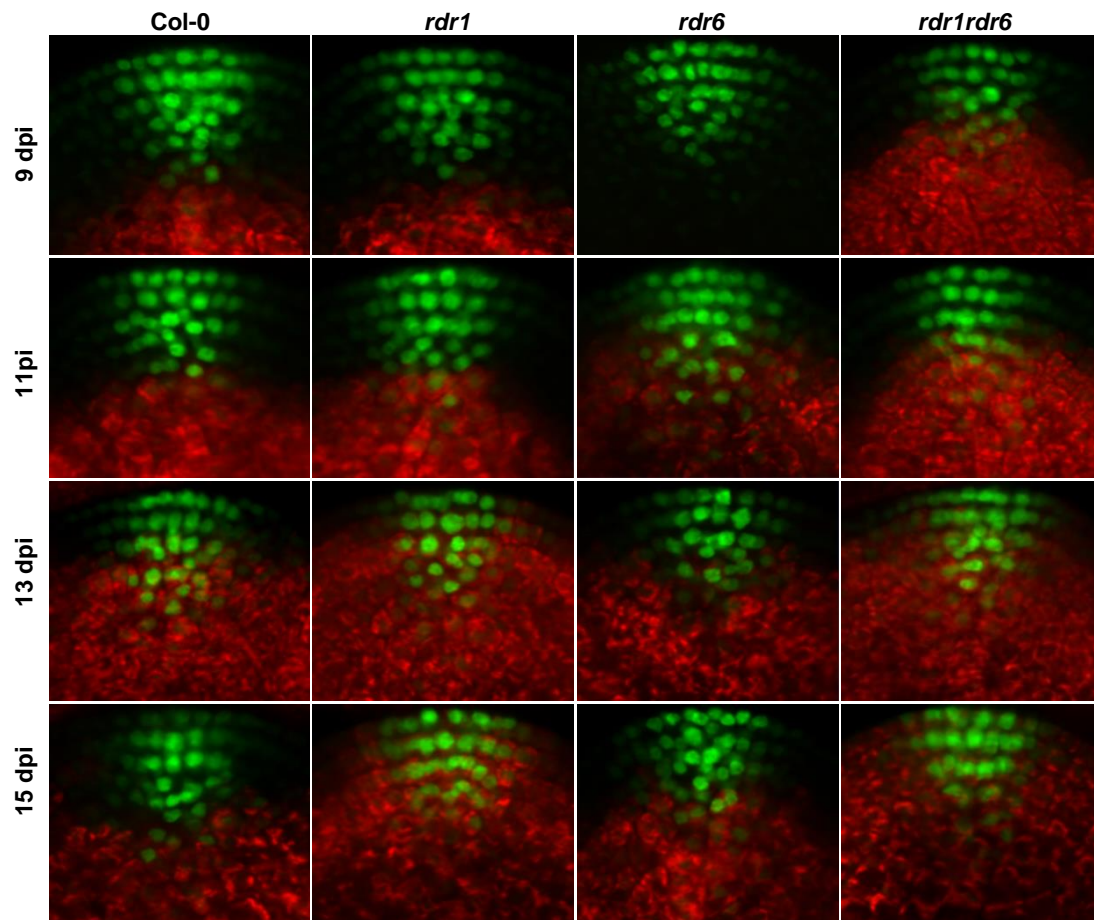


Fig. 7: **Acquisitions of meristems at different timepoints and genotypes.** Green fluorescence protein is expressed in the meristem. Red fluorescent protein labels TuMV-infected cells.

At 9 dpi, the TuMV infection front was already close to the meristem dome (25-30  $\mu\text{m}$  from the tip) in all genotypes. Notably, TuMV appeared to arrive at this point slightly more slowly in the *rdr6* mutant.

At 11 dpi, TuMV had almost completely invaded the meristem in *rdr1rdr6*, with very high levels of fluorescence throughout, while in the *rdr1* mutant it had progressed up to the L2. In *rdr6*, the red TuMV distribution in relation to the L1-L3 layers was similar to wild type, albeit showing greater red fluorescence in lower cell layers.

At 13 dpi, TuMV in *rdr1* showed a distribution analogous to *rdr1rdr6*, invading all cell layers of the meristem, including the L1. By contrast, *rdr6* plants showed similar patterns as wild type, with TuMV entering the L3 layer. Low levels of TuMV were observable in the L1 and L2 in *rdr6* and wild type.

At 15 dpi, the infection patterns stayed mostly the same in all genotypes.

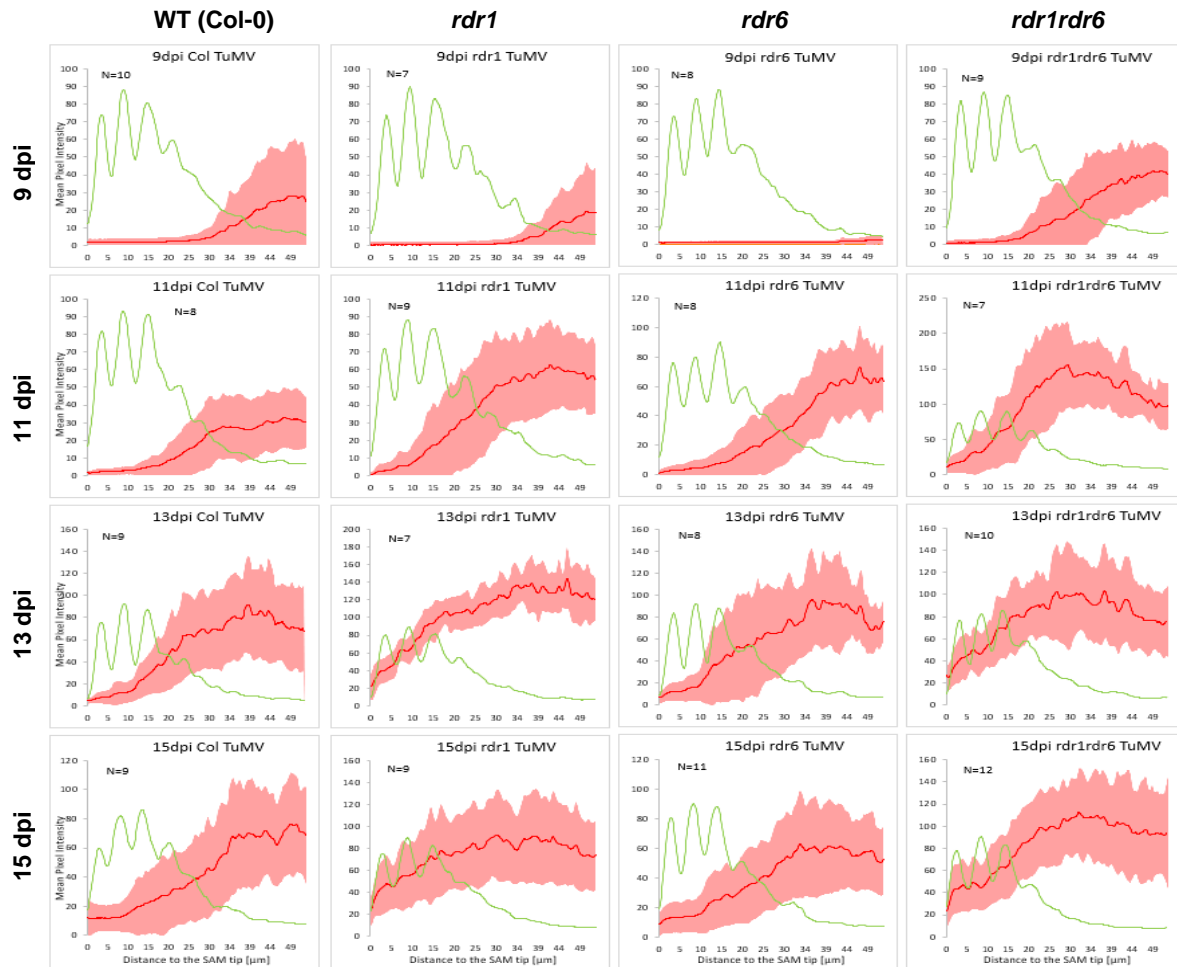


**Fig. 8: Quantification of virus entry into the meristem in WT and RDR mutants.** The average mean red pixel intensity (red line) 0 to 50  $\mu\text{m}$  from the meristem tip of several meristems for each genotype per timepoint indicates the presence of TuMV-6K2:Scarlet. The red zone around the line indicates deviation between samples with one degree of standard deviation up and down. The average mean green pixel intensity (green line) of the corresponding meristems indicates the position of the cell layers from the L1 to the L3, as the signal comes from the nuclei labeled with pCLV3::H2B-Clover. N = number of individual meristems analyzed.

To compare TuMV-derived red fluorescent protein accumulation (referred to as virus load hereafter) in the different genotypes, the area under the mean red pixel intensity curves from 0 to 50  $\mu\text{m}$  of the meristem tip was integrated (Figure 9). Both Col-0 and *rdr6* exhibited mean maximum relative virus loads of 2500-2900 at 13 dpi. *rdr1* and *rdr1rdr6* showed higher mean maximum relative virus loads of 4900-5200, with *rdr1* reaching its maximum at 13 dpi as well and *rdr1rdr6* peaking earlier at 11 dpi.

Hence, *RDR1* does not only play an important role in the exclusion of TuMV from the stem cells, but has an influence on the overall virus load in the lower layers of the meristem dome. Particularly in the *rdr1rdr6* double mutant, the speed of virus movement appears to be elevated. Although in literature *RDR6* was often highlighted as a vital factor in virus meristem exclusion in *Nicotiana benthamiana* (Schwach et al., 2005; Di Serio et al., 2010; Qu et al., 2020), virus movement speed, virus location, and virus load in the single *rdr6* *A. thaliana* mutant was very similar to that in the Col-0 wild type. Overall, the data indicate that *RDR1* is responsible for the exclusion of TuMV from the meristematic stem cells, while *RDR6* is able to temporarily prevent virus invasion in the absence of *RDR1*.

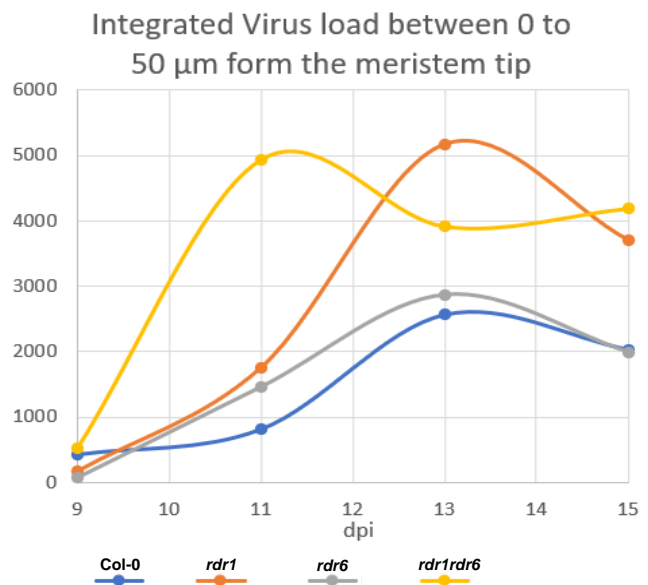


Fig. 9: **Relative TuMV virus load in the different genotypes at different dpi.** The mean red pixel intensities in Figure 8 were integrated between 0 to 50 µm from the meristem tip, representing here the mean total virus load in this area.

#### 4.2) TuMV infection dynamics with daily resolution in Col-0 and *rdr1* (10-18 dpi)

To obtain a better understanding of the precise dynamics behind the phenomenon of TuMV meristem exclusion, and in particular to better understand the role of *RDR1*, another time-course experiment was performed, acquiring images of Col-0 and *rdr1* SAMs every day between 10 to 18 dpi. 7-12 meristems per timepoint and genotype were analyzed (indicated with N in Fig. 10). The general workflow and procedures were the same as in the previous experiment. The state of invasion into the meristem at different timepoints can be seen in Fig. 10. The infection dynamics broadly reflect those observed

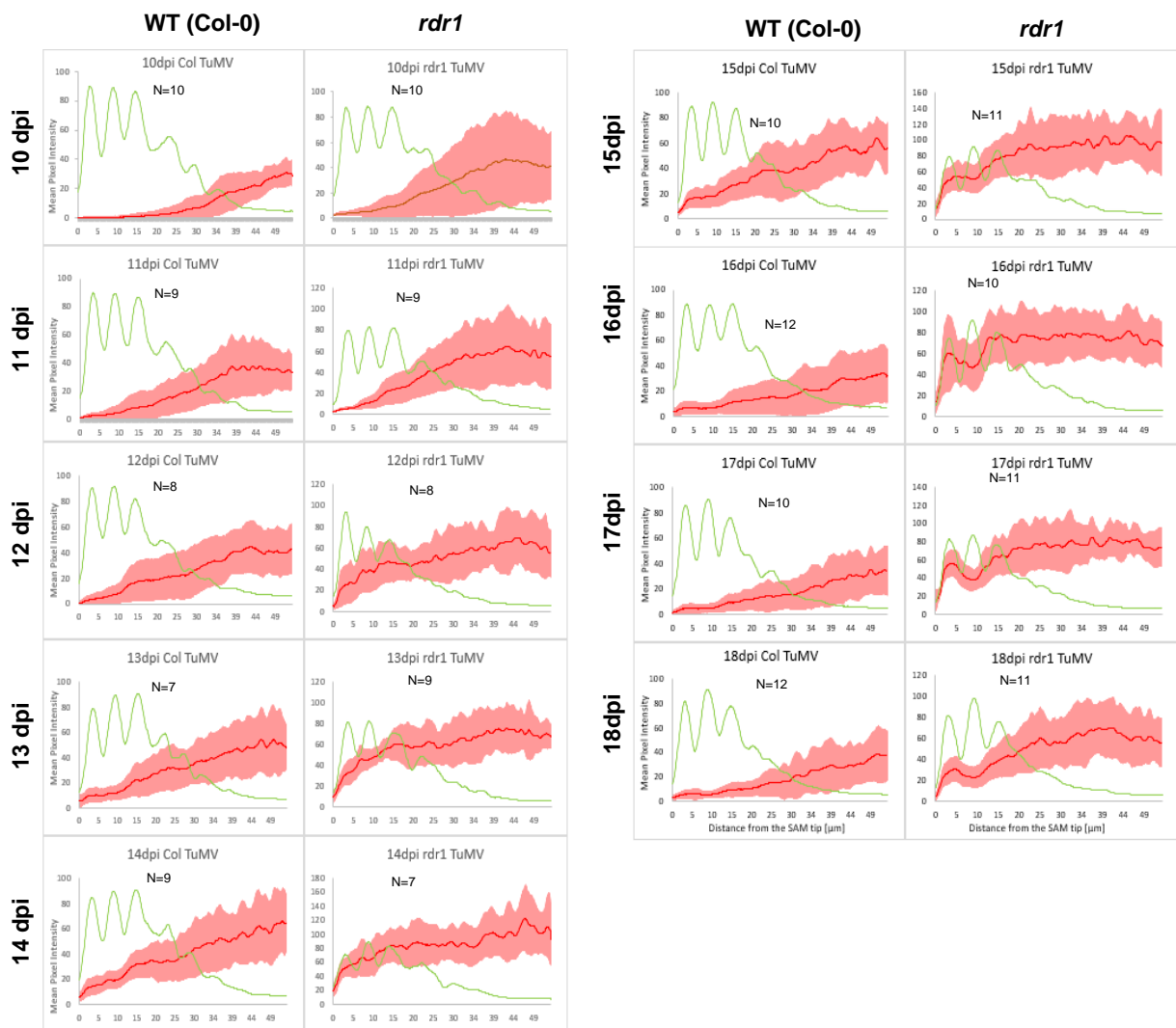


Fig.10: **Daily progress of TuMV infection in the meristems of Col-0 and *rdr1* plants from 10 to 18 dpi.** The average mean red pixel intensity (red line) from 0 to 50  $\mu\text{m}$  from the meristem tip of several meristems for each genotype per timepoint indicates the presence of TuMV-6K2:Scarlet. The red zone around the line indicates deviation between samples with one degree of standard deviation above and below. The average mean green pixel intensity (green line) of the corresponding meristems indicates the position of the cell layers from the L1 to the L3, as the signal comes from the nuclei labeled with pCLV3::H2B-Clover. N = number of individual meristems analyzed.

in the previous experiment (Fig. 8), attesting to their reproducibility. In wild type Col-0 plants, TuMV can be observed to accumulate at low levels in the L1-L3 layers between 13-15 dpi, only to return to basal levels at later time points. This suggests that the phenomenon of TuMV meristem exclusion follows only after transient entry into the stem cells. In *rdr1*, TuMV enters the stem cells earlier, at 11-12 dpi, and results in dramatically higher levels of fluorescence in these cell layers, most likely a consequence of greatly increased virus replication and/or translation. Interestingly, also in *rdr1* the virus-derived fluorescence declines in the stem cells after reaching a peak around 14-15 dpi, suggesting that *RDR1*-independent antiviral mechanisms are active as well. Notably, a decrease in virus fluorescence can be observed in *rdr1* at later time points, specifically in the L2 compared to L1 and L3. To better assess TuMV invasion of the L1 and L2 stem cell layers, I plotted the fluorescence signals in these two cell layers separately (Fig. 11). This analysis reiterates the extensive difference in TuMV dynamics between WT and *rdr1* mutants, stressing the importance of RDR1 in stem cell-specific antiviral defense. This analysis also clearly confirms the decrease in TuMV-derived fluorescence at later time points in *rdr1*. This decrease however seems to have been ongoing at 18 dpi. Therefore, to extend the observation period during later time points, I conducted another TuMV infection time course experiment, in which I observed WT and *rdr1* plant meristems from 17 to 23 dpi.

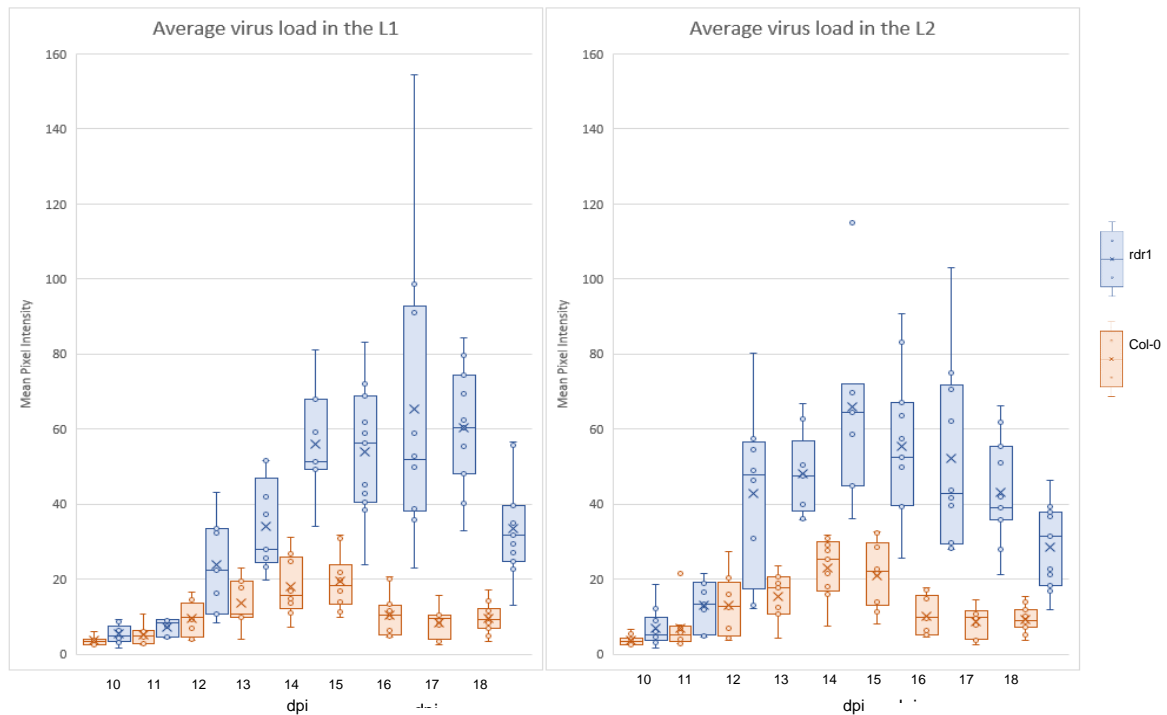


Fig. 11: Quantification of transient virus presence in the L1 and the L2 of WT (Col-0, orange) and *rdr1* (blue) from 10 to 18 dpi. For image acquisition and processing see legends to Fig. 8 and 10.

### 4.3) Later TuMV infection dynamics in Col-0 and *rdr1* (17-23 dpi)

An additional time course experiment with the previous set-up, but from 17-23 dpi was conducted to determine the virus load in the *rdr1* mutant at later time points (Fig. 12). The fluorescence levels measured at 17-18 dpi, especially in *rdr1*, reflect those observed at 15-16 dpi in the previous experiment (Fig. 10), suggesting a slower progression of infection in this experiment. At these later time points, red fluorescence remained at basal levels in Col-0, as expected. In *rdr1*, after a peak of fluorescence in the stem cells at 17-18 dpi, virus fluorescence persisted in these cells, with reduced fluorescence specifically in the L2. Over these time points there was a prominent decline in red fluorescence in the stem cells, though the values remained higher than in WT. Analysis of the virus fluorescence levels in the L1 and L2 confirms that in *rdr1*, TuMV load decreased in stem cells at later time points (Fig. 13). Extrapolating this trend in virus regression in *rdr1* suggests that the fluorescence levels could eventually reach that of the wild type. However, with the data at hand it is not possible to test this hypothesis.

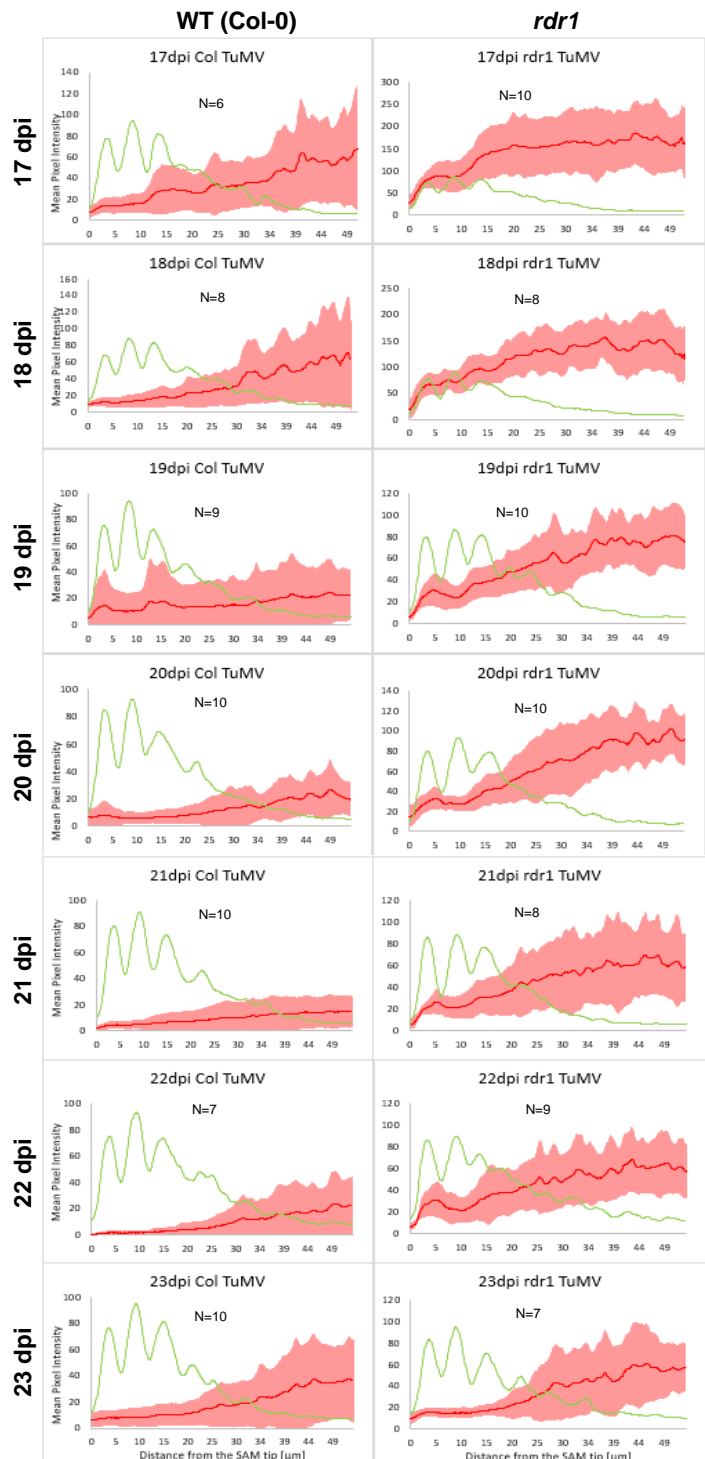


Fig. 12: **Time course of progressing TuMV infection into the meristems of Col-0 and *rdr1* plants from 17 to 23 dpi.** In green the mean green pixel intensities of the CLV3 meristem reporter. In red the mean red pixel intensities of virus fluorescence. For each timepoint and genotype, N meristems were observed and averaged.

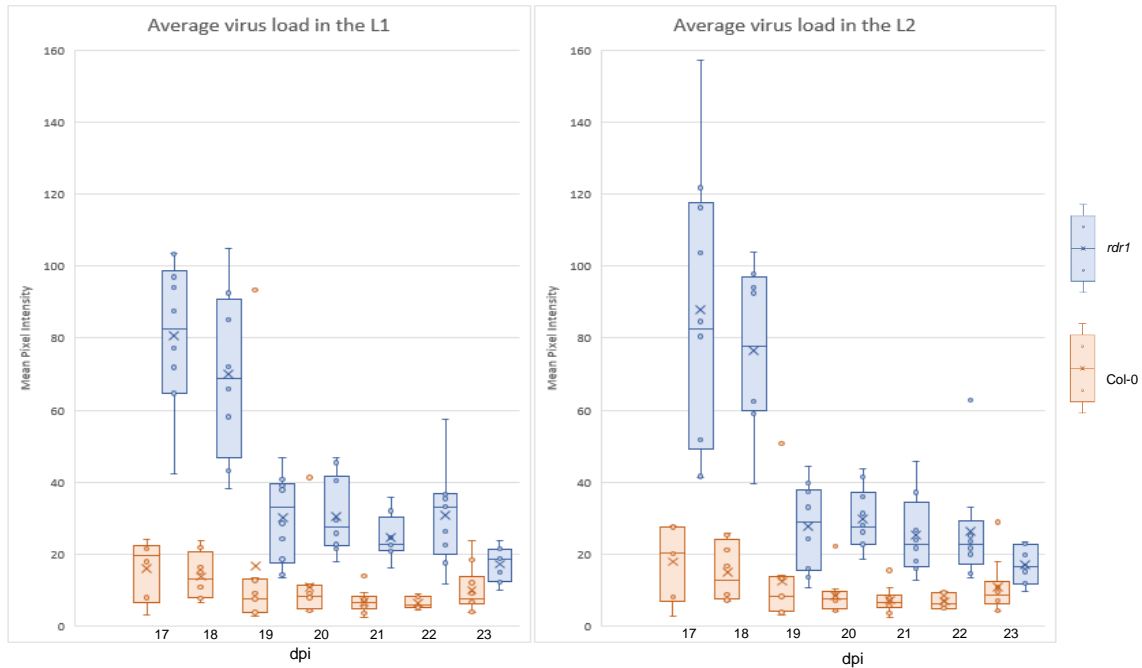


Fig. 13: Quantification of transient virus presence in the L1 and the L2 of WT (Col-0, orange) and *rdr1* (blue) from 17 to 23 dpi. For image acquisition and processing see legends to Fig. 8 and 10.

Next, we wondered whether *RDR1* could have a non-meristem specific anti-viral effect, causing systemically higher virus loads in the *rdr1* mutant. When the virus infection front would reach the SAM, this could saturate the defense mechanisms and hence indirectly enable temporary invasion of the meristem. To test whether this would be the case, TuMV genomic RNA levels were quantified in shoot apices via RT-qPCR at 11 dpi (Fig. 14). As virus accumulation did not vary in Col-0 and *rdr1*, this hypothesis could be excluded.

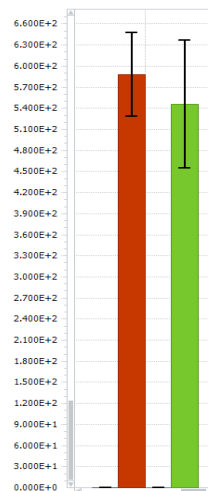


Fig. 14: Relative accumulation levels of TuMV RNA in Col-0 and *rdr1* plants infected and mock-infected. Red: Col-0 infected, Green: *rdr1* infected. Relative expression levels were normalized to the AtSand gene (At2G28390).

#### 4.4) TuMV infection dynamics in Col-0 and *dcl2dcl3dcl4*

To test whether the virus load regression in *rdr1* depends on other compounds of the silencing pathway, a time course experiment was conducted in the *dcl2dcl3dcl4* triple mutant. *DCL2* and *DCL4* are known to be crucial in the production of primary vsRNAs (Guo et al., 2018), and therefore are putatively both upstream and downstream of *rdr1*. Col-0 and *dcl2dcl3dcl4* plants were infected in the same manner as in the previous experiments, and meristems observed at 9, 11, 13, 15 and 17 dpi. Plants and TuMV carried the same fluorescence reporters as in the experiments described above.

Infection dynamics in Col-0 were consistent with previous experiments. In contrast to the infection in the *rdr1* mutant, TuMV steadily increased in the L1 and L2 of *dcl2dcl3dcl4* mutants, without apparently reaching a peak before diminishing as in *rdr1* (Fig. 15 and 16). To establish whether the

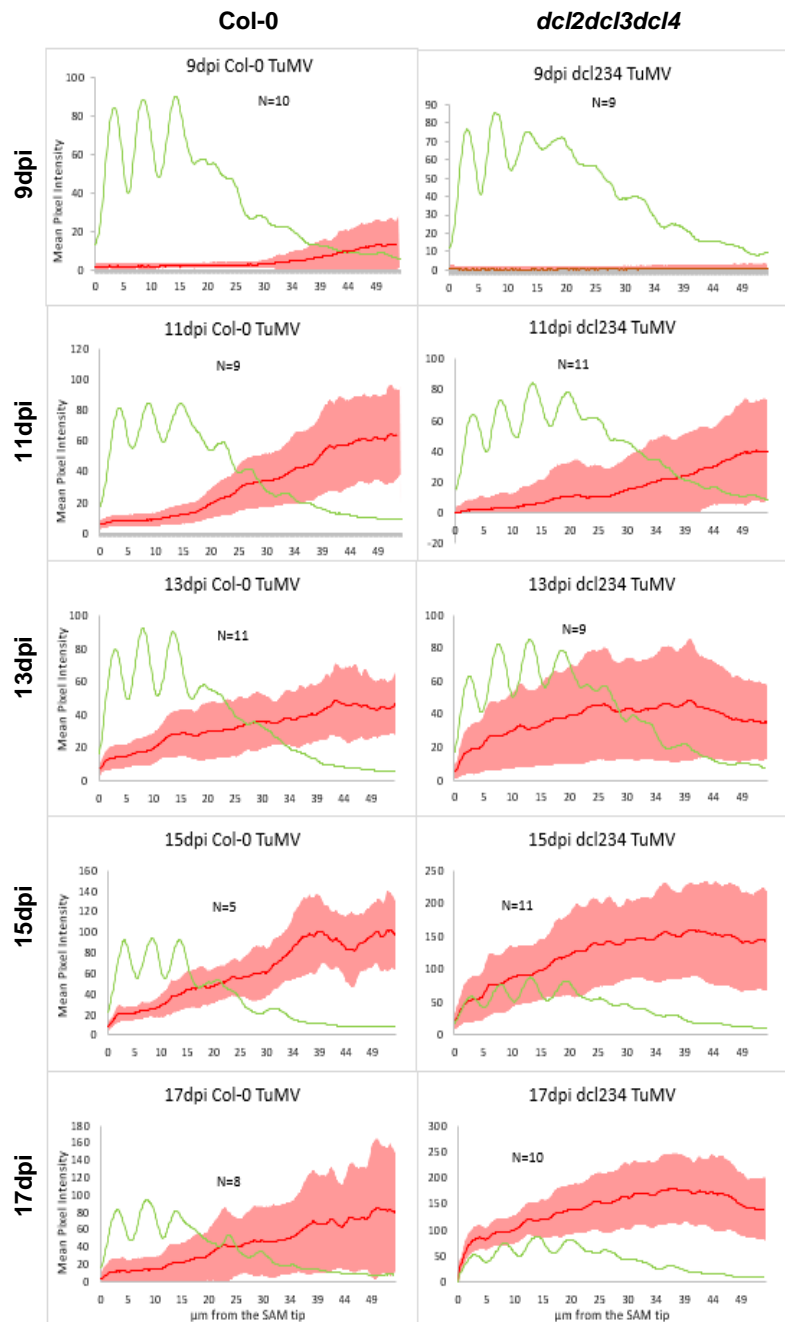


Fig. 15: Time course of TuMV infection into the meristems of Col-0 and *dcl2dcl3dcl4* plants. In green the mean pixel intensities of green fluorescence of the CLV3 meristem reporter. In red the mean pixel intensities of red virus fluorescence. For each timepoint and genotype, N meristems were observed and averaged for the graphs at 9 to 17 dpi, every other day.

red fluorescence would persist on a high level or would decline at later time points could not be answered without another time course experiment. Theoretically, if virus levels remained at high levels, without showing the subsequent decline observed in *rdr1*, one or more RNAi-dependent mechanism could be in place that are independent of *RDR1*, but still downstream of *DCL2*, *DCL3* and *DCL4*. On the other hand, declining virus levels at later time points could suggest that another, siRNA-independent mechanism is also counteracting virus meristem invasion. These possibilities are not mutually exclusive. At 17 dpi, the phenomenon of lower virus load in the L2, clearly visible in *rdr1*, could not be observed in *dcl2dcl3dcl4*, suggesting that antiviral RNAi mechanisms independent of *RDR1* are active in this important cell layer. Observation of later time points would be of great interest in the future.

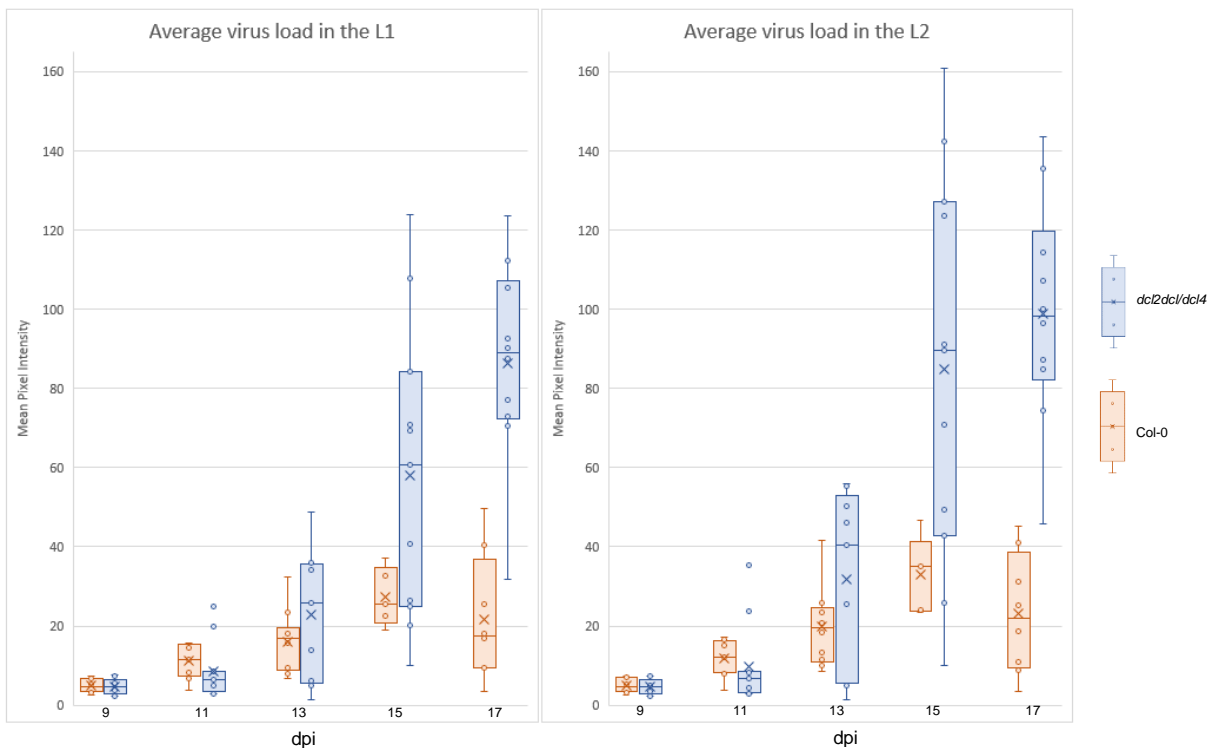


Fig. 16: Quantification of transient virus presence in the L1 and the L2 of WT (Col-0, orange) and *dcl2dcl3dcl4* (blue) from 9 to 17 dpi. For image acquisition and processing see legends to Fig. 8 and 10.

#### 4.5) RDR1 is expressed in the stem parenchyma and leaf vasculature

To evaluate the site of expression of RDR1, transcriptional reporter lines, expressing a green fluorescent protein fused to the H2B histone under the RDR1 promoter (Col-0/pRDR1::H2B-Clover) were used. From TuMV- or mock-infected plants, meristem, stem, and leaf tissues were sampled 14 dpi and analyzed with a confocal point-scanning microscope. In mock-infected plants, green nuclei – indicating expression driven by the RDR1 promoter – were evenly distributed in the parenchyma of stem tissue, including the vasculature of the plant (Fig. 17). However, no green fluorescence was observed in

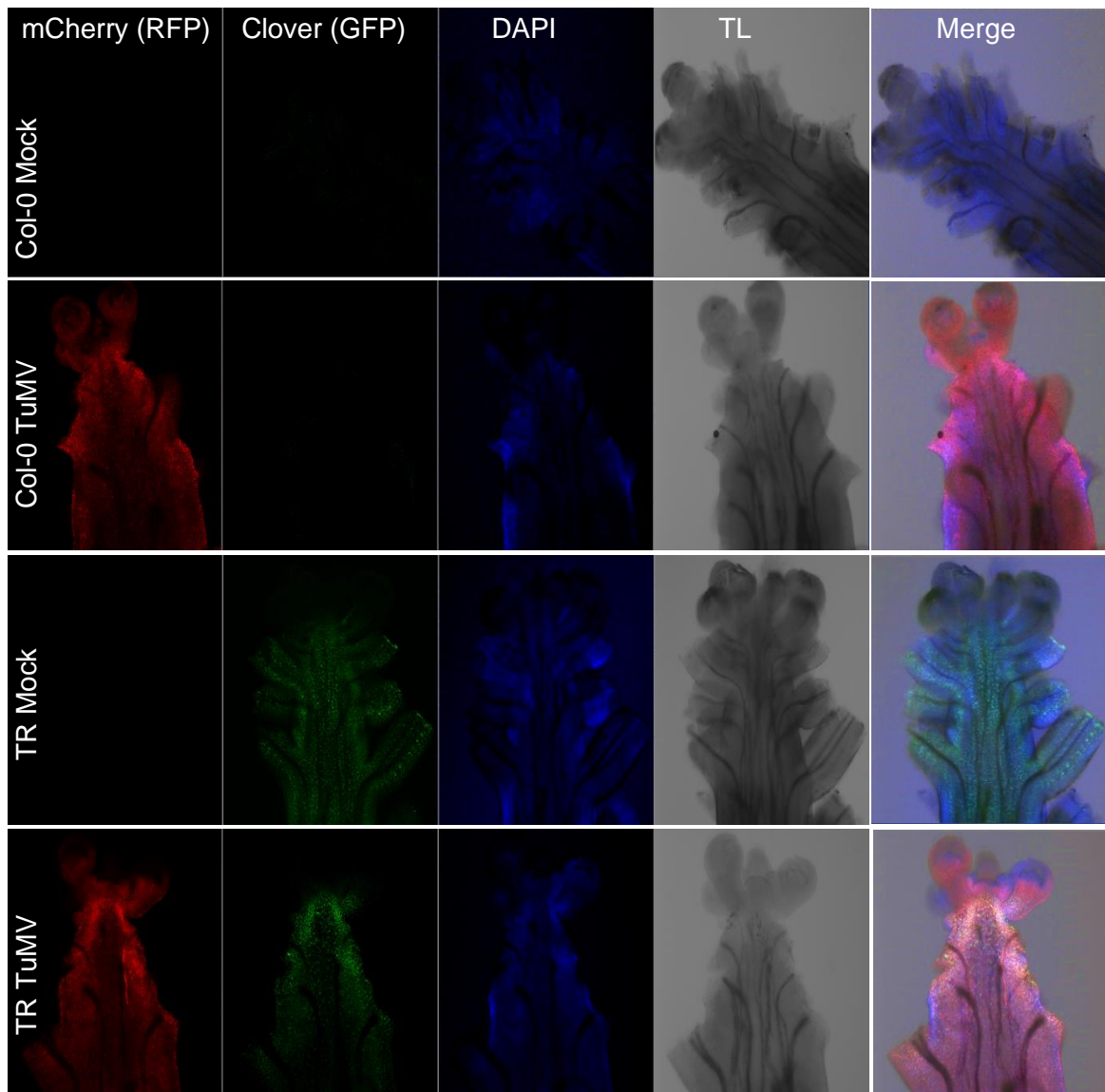
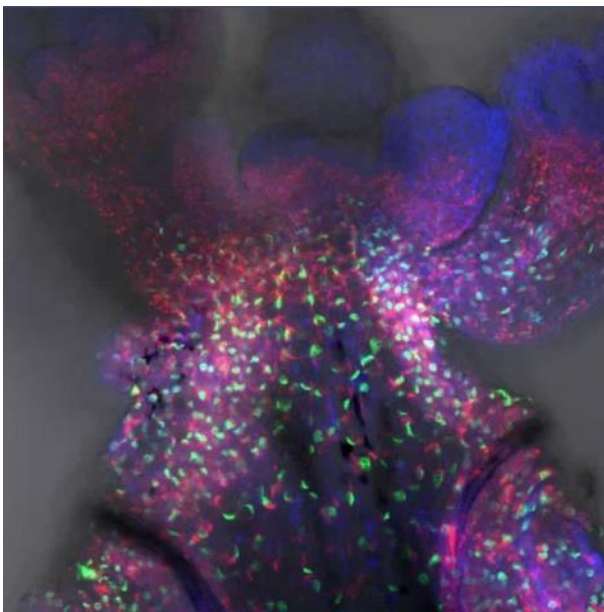


Fig. 17: **Expression pattern of RDR1 in apical shoot meristems of mock- or TuMV-infected plants at 14 dpi.** Fluorescence channels from left to right: Red (virus), green (RDR1), blue (DAPI), transmitted light (TL), merged images. Col-0 mock- or TuMV-infected (row 1 and 2), *RDR1* transcriptional reporter (TR) mock- or TuMV-infected (row 3 and 4).

the meristem or the flower buds (Fig. 17 & 18). Upon infection with TuMV-6K2:Scarlet, the site of H2B:Clover expression did not change, but was stronger at sites with higher virus load in the basal proximity of the SAM at 14 dpi (Fig. 17). Even though TuMV was also replicating in the flower buds at 14 dpi, *RDR1* was not expressed in this tissue (Fig. 17 & 18). Therefore, the *RDR1* promoter drives expression either specifically below the meristem upon TuMV infection, or generally at the front of infection where TuMV replication and translation is likely most active. To distinguish between these alternatives, it would be interesting to look at earlier timepoints during the infection of these *RDR1* reporter lines, when the virus infection front has not yet reached the meristem.



**Fig. 18: Close-up expression pattern of the *RDR1* promoter around the meristem of a TuMV-infected plant.** Merged image with fluorescent nuclei in green, TuMV in red, DAPI in blue.

As H2B:Clover is not visibly expressed in the meristem upon infection, it is possible that either *RDR1* products – presumably siRNAs – or the *RDR1* protein itself moves into the meristem and establishes the exclusion of the virus. In leaves, *RDR1* is expressed in the vasculature, with no notable change in the site or level of expression upon TuMV infection (Fig. 19). Generally, these findings correspond very well with the literature describing *AtRDR1* expression predominantly focused around the vasculature and little expression in meristematic tissue (Xu et al., 2013). Due to only weak

expression of the reporter gene in the leaves of transcriptional reporter lines, high laser intensities for the excitation of green fluorescence had to be used at the confocal microscope. Due to the partial overlap in excitation spectrum of Scarlet (RFP) and Clover (GFP), this resulted in false fluorescence in the green channel of Col-0 TuMV (Fig. 19, second row and column).

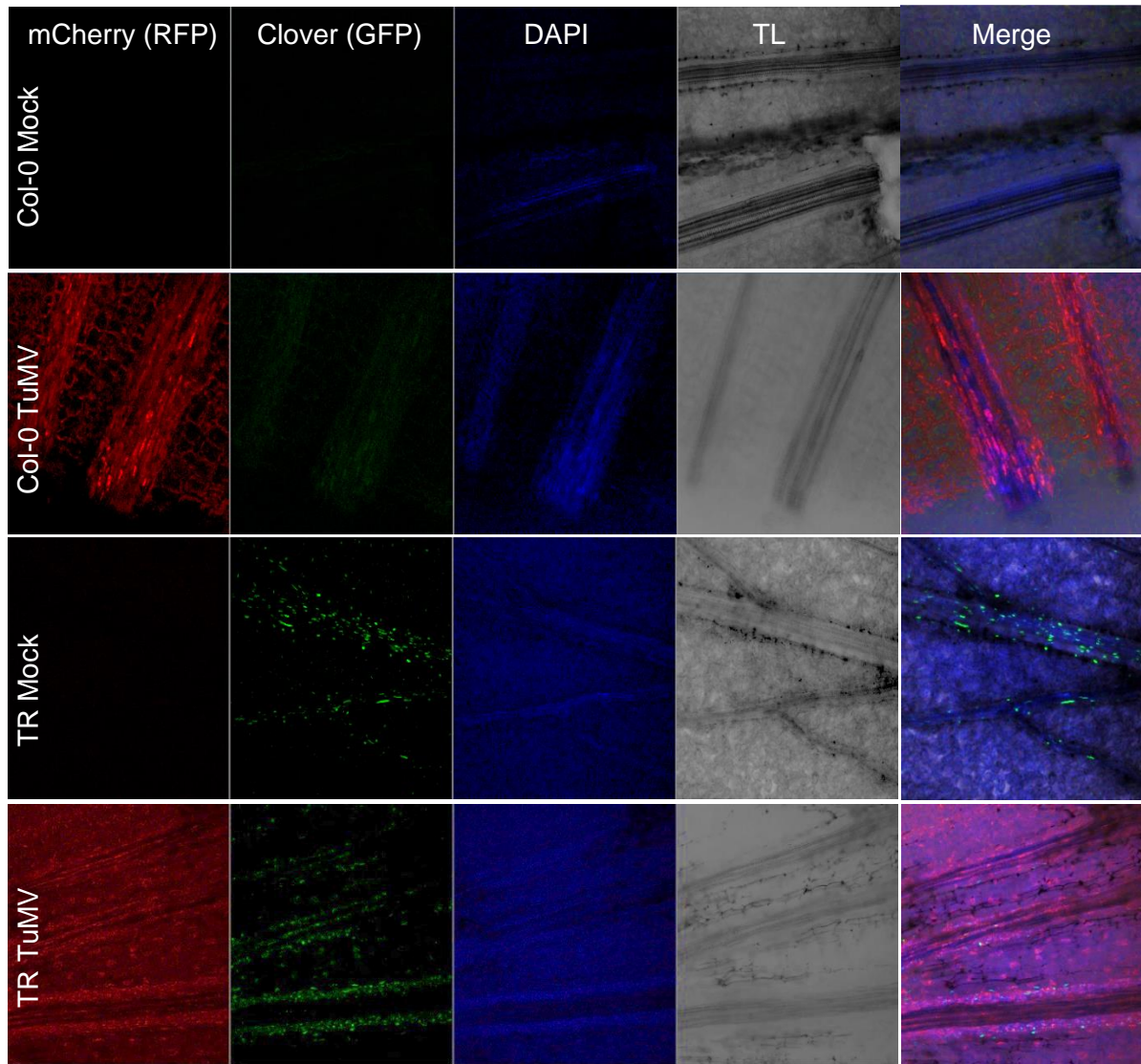


Fig. 19: **Expression pattern of the *RDR1* promoter in leaves of mock- and TuMV-infected plants.** Fluorescence channels from left to right: Red (TuMV), green (pRDR1:H2BClover), blue (DAPI), transmitted light (TL), merged images. Col-0 mock- or TuMV-infected (row 1 and 2), *RDR1* transcriptional reporter (TR) mock- or TuMV-infected (row 3 and 4).

#### 4.6) Role of RDR1-produced vasiRNAs

To investigate the role of vasiRNAs during virus infection, RNA was extracted from the inflorescences of mock- or TuMV-infected *A. thaliana* Col-0 and *rdr1* plants at 11 dpi. cDNA was generated and used for RT-qPCRs including the *AtSAND* (*At2G28390*) house-keeping gene for normalization, to evaluate the transcript levels of several endogenous genes that are supposedly targeted by vasiRNAs during TuMV infection. I chose to analyze transcript levels of *LHCb1.3*, *At5G201700*, *HSP70-1* and *NBR1*, as the first three were shown to be down-regulated by vasiRNAs during CMV infection (Cao et al., 2014). Specifically, I chose to evaluate *NBR1* transcript levels, as it is the gene with the most annotated vasiRNAs during TuMV infection (Cao et al., 2014). All genes were either up- or down-regulated to a similar extent in Col-0 and *rdr1* during infection (Fig. 20). Therefore, no evidence for vasiRNA-dependent regulation of these genes was found in two independently performed experiments on the same biological material (replicate not shown). Thus, the transcripts were probably not targeted by the vasiRNAs for degradation. This could be due to the fact that TuMV has a functional VSR (HC-Pro) that is able to suppress vasiRNA-dependent silencing, whereas CMV- $\Delta$ 2b used in the cited study (Cao et al., 2014) lacks its VSR 2b. *RDR1* is induced about 1.5-fold upon infection in the tissues analyzed. The low transcript levels of *RDR1* in the infected *rdr1* mutant are likely derived from a DNA contamination during the cDNA preparation (Fig. 20).

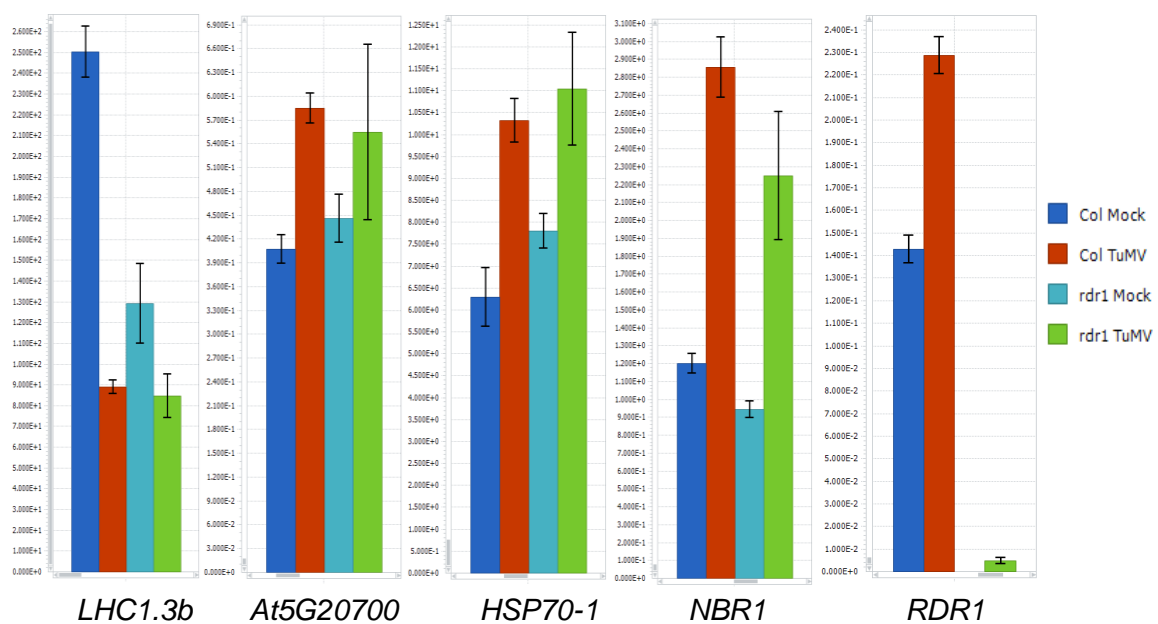


Fig. 20: **Transcript levels of different genes evaluated via RT-qPCR.** Transcript levels of four potential vasiRNA target genes and *RDR1* were analyzed in Col-0 and *rdr1*, mock- or TuMV- infected plants.

To see whether the vasiRNAs could nonetheless act as regulators on a translational level, protein was extracted from the shoot tip of mock- and TuMV infected *A. thaliana* and a Western blot was performed to quantify the NBR1 protein. Even though the NBR1 levels were strongly increased upon infection, this occurred in an RDR1-independent manner (Fig. 21).

Hence, changes in gene expression of vasiRNA targeted genes that have been observed in *A. thaliana* upon CMV- $\Delta$ 2b infection (Cao et al., 2014) have not been observed upon TuMV infection, likely for the reasons mentioned above.

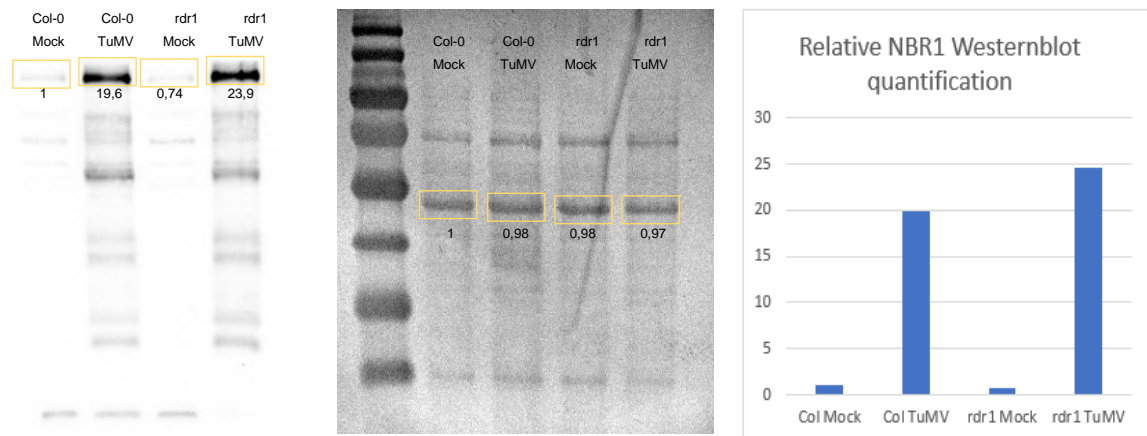


Fig. 21: **Western blot of NBR1 proteins in Col-0 and *rdr1*, mock- and TuMV-infected.** Left: Membrane for immunodetection with  $\alpha$ -NBR1 antibodies. Middle: Coomassie-stained Western blot membrane as a control for equal loading. Right: Relative quantification of NBR1 protein levels based on signal intensities in the Western blot.

## 5) Discussion

The novel method used in this thesis to quantify virus meristem invasion in different cell layers over a period of time proved to be a powerful tool to analyze this phenomenon. In my time-course experiments I consistently demonstrated that prior to the exclusion of TuMV from the SAM of wild type plants there is a period of several days when the virus transiently enters the meristem and accumulates therein. Furthermore, I demonstrated for the first time the vital role of *RDR1* in the exclusion of TuMV from the SAM of *A. thaliana*, and I precisely described its dynamics. I show that TuMV can drastically invade all layers of the SAM in *rdr1* plants, but that the protection granted by RDR1 is likely limited to a period of around two weeks in our experimental conditions. These experiments also show that the roles of RDR6 and the DCL proteins in TuMV meristem exclusion can be spatially and temporally resolved, demonstrating the existence of a multi-layered RNAi-dependent set of antiviral defenses. This work emphasizes how important it is to analyze highly dynamic processes like the ongoing infection with adequate methodology, when technically feasible.

### 5.1) Possible explanations for TuMV meristem exclusion dynamics in *rdr1* plants

Generally, virus-dependent fluorescence in the meristem tip was about three times higher in *rdr1* mutants than in Col-0 and reaching its peak two to three days later than in Col-0. From 20 to 23 dpi on, TuMV levels in *rdr1* mutants were progressively nearing those in Col-0, but remained higher. With the data at hand, it is unclear if at even later timepoints virus load would be the same in both genotypes.

Considering the steady increase in virus accumulation until 17 dpi in the *dcl2dcl3dcl4* triple mutant time-course, it would be informative to know how the infection would proceed in this genotype at later timepoints. Either virus levels would stagnate, or – similarly to Col-0 and *rdr1* genotypes – would decline again. Hypothetically, if virus levels in the *dcl2dcl3dcl4* mutant declined at later timepoints, it would suggest an RNAi-independent mechanism at work. On the other hand, hypothesizing that virus accumulation in *dcl2dcl3dcl4* would stagnate at a high level, it could mean several models for the function of *RDR1* in the exclusion of virus from the meristem: (1) *RDR1* could play an essential role especially in the early stages of meristem invasion as a quick responder, but after several days is superseded by other mechanisms that are *RDR1*-independent. (2) *RDR6* could take over the role in the production of secondary vsRNAs.

It could be less efficient in doing so, and therefore temporarily allow higher TuMV accumulation in the SAM. Further explanations for the possible role of RDR6 can be found under the point 4.4.

To test hypothesis nr. 2, a detailed time course with the *rdr1rdr6* double mutant would be interesting. In the *rdr1rdr6* double mutant, TuMV reached the SAM faster, but generally accumulation levels and mean red pixel intensity curves were similar to that of the *rdr1* mutant. But as the latest timepoint observed in the experiments that included the *rdr1rdr6* mutants was 15 dpi, it remains unclear whether virus load in the meristem would also decline in this mutant later or not. If TuMV levels do not decline in *rdr1rdr6* meristematic domes at later timepoints, it would suggest that the exclusion of TuMV is established by *RDR1*- and *RDR6*-dependent secondary vsRNAs. On the other hand, if TuMV levels decline in the *rdr1rdr6* double mutant (but not in the *dcl2dcl3dcl4* triple mutant), it could also mean that either *DCL2*- and/or *DCL4*-derived primary vsRNAs are sufficient to again eliminate the viruses from the meristematic dome.

To answer questions that have arisen from my results, I propose to perform a prolonged and detailed version of the *dcl2dcl3dcl4* time-course experiment. If virus levels in this *dcl2dcl3dcl4* experiment stagnate in the SAM without showing a decline at later timepoints, I further would propose to perform a prolonged and detailed version of the *rdr1rdr6* time-course experiment. These two experiments should shed further light on the roles of primary vsRNAs and the role of RDR6 in the exclusion of TuMV from the meristem, in particular at later timepoints of infection.

## 5.2) Virus load in Col-0 and *rdr1* plants

Interestingly, by evaluating the virus load in the shoot tip and flower buds of Col-0 and *rdr1* via RT-qPCR, I showed that virus load was comparable in both genotypes at 11 dpi. For this experiment I had sampled the inflorescences with approximately one centimeter of stem. On the contrary, when evaluating the virus load by integrating the mean red fluorescence pixel intensity curves from 0 to 50  $\mu\text{m}$  from the meristem tip of infected Col-0 and *rdr1* plants, I obtained almost twice the virus load in the *rdr1* mutant when compared to Col-0. Therefore, in the *rdr1* mutants, TuMV could specifically accumulate to a higher extent in and closely adjacent to the SAM. In more basal regions and in flower buds, however, there seems to be no real difference in virus accumulation. Some studies have reported substantial differences in virus load in *rdr1* mutants and wild type (Wang

et al., 2010; Cao et al., 2014). However, in these studies they used viruses lacking a VSRs, which makes their behavior non-representative of the fully functional virus. Of course, we cannot exclude that the values of scarlet fluorescence (microscopy measurements) and TuMV gRNA accumulation (RT-qPCR) are not always proportional, meaning that red fluorescence cannot always be used to precisely estimate virion accumulation. Nevertheless, it is a good proxy to visualize virus movement and translation.

### 5.3) Lower virus concentration in the L2 of *rdr1* plants

An interesting observation was the drop of virus-derived red fluorescence in the L2 of infected *rdr1* plants at 17 dpi to 22 dpi. This was consistently observed in both time-course experiments that covered these timepoints. As the L2 gives rise to the germline and gametes (Burian, 2021), it is remarkable that this cell layer seems to be under particularly tight virus control. This mechanism must be *RDR1*-independent, as it was especially observable in *rdr1* mutants. Interestingly, this phenomenon did not occur at 17 dpi in the *dcl2dcl3dcl4* mutants, suggesting that it is *RDR1*-independent but siRNA-dependent. However, even though results of individual time-course experiments were reproducible and consistent within an experiment, the progression of virus infection patterns showed shifts of up to two days when compared to other time-course experiments. Therefore, it cannot be excluded that the phenomenon of lower virus concentration would still have occurred in the L2 of *dcl2dcl3dcl4* plants. A prolonged and more refined version of the *dcl2dcl3dcl4* time-course experiment (covering for example 15 to 23 dpi on a daily basis) again could offer a more comprehensive picture.

### 5.4) *RDR6* and its role in virus meristem exclusion

Not much is known concerning the role of *AtRDR6* in the exclusion of virus from the SAM of *A. thaliana*. Its role might be virus species-dependent; as it is claimed that knocking out *RDR6* in *A. thaliana* results in a higher susceptibility against *Cucumber mosaic virus* (CMV), whereas susceptibility against TuMV or *Turnip vein-clearing virus* (TVCV) is unaffected (Mourrain et al., 2000). This correlates well with my observation that TuMV exhibits similar progression dynamics in *rdr6* mutants and Col-0, indicating that *RDR6* seems not to play a role in the exclusion of TuMV from the SAM of *A. thaliana*. However, the *rdr1rdr6* double mutant allowed a faster virus invasion. Therefore, during TuMV

infection, *RDR6* – even though unable to exhibit recognizable antiviral effects on its own – might be able to slow virus progression when acting in combination with *RDR1*.

Generally, studies on *Nicotiana benthamiana* have shown that *NbRDR6* is essential to inhibit meristem invasion of *Potato virus X* (PVX) and *Potato spindle tuber viroid* (PSTVd) (Schwach et al., 2005; Di Serio et al., 2010; Qu, et al., 2005). As *N. benthamiana* has no *AtRDR1* homologue (Ying et al., 2010), it could be that the importance of *NbRDR6* in virus meristem exclusion is elevated.

### 5.5) Role of TuMV induced vasiRNAs and NBR1 in virus resistance

It has been shown that upon TuMV infection of *A. thaliana*, vasiRNAs (siRNAs annotated to exons of host-encoded genes) are produced in an *RDR1*-dependent manner; with the most represented gene in vasiRNA sequences being *NBR1* (Cao, et al., 2014). In this study the authors showed that vasiRNAs produced during CMV- $\Delta$ 2b infection down-regulate the corresponding host genes. In this thesis, I showed that genes that were proposed by Cao et al. (2014) to be targeted by vasiRNAs upon TuMV infection in *A. thaliana* (including *NBR1*) are rather up-regulated (the exception being *LHC1.3b*). Here, during infection by TuMV with its strong VSR (HC-Pro), endogenous gene silencing might not be possible to be established. An obvious explanation for the down-regulation in the cited study might be the deficiency of CMV- $\Delta$ 2b, lacking its VSR, so that vasiRNAs could trigger degradation of their target. As the authors did not show whether a regulatory effect is exhibited in fully functional viruses, it is not clear if vasiRNAs act directly upon the regulation of gene expression during infection. However, in another study, supporting the data of Cao et al. (2014) three plant species of the Brassicaceae family (namely *A. thaliana*, *Brassica rapa* and *Brassica napus*) were infected with wild type *Cauliflower mosaic virus* (CaMV). The targeted genes corresponded well with the genes targeted in the study of Cao et al. (2014), and were shown to be downregulated likewise (Leonetti et al., 2020). This seems contradicting to the data provided in this thesis. It is hard to tell though, if the VSR of CaMV, P6, is rather strong or weak in comparison to HC-Pro. If antiviral silencing is only weakly suppressed by P6, the phenotype of vasiRNA production might resemble that of the infection with the VSR-deficient CMV-  $\Delta$ 2b used by Cao et al. (2014). These differences in separate observations further highlight how different virus species in different hosts trigger very different post-transcriptional cascades.

*Atnbr1* mutants showed an elevated resilience against TuMV infection, exhibiting less

virus accumulation and symptoms (Li et al., 2020). A downregulation of NBR1 upon infection therefore could be advantageous for the plant. On the other hand, there is contradicting evidence that *Atnbr1* mutant plants are more susceptible to TuMV and accumulate more virus (Hafrén et al., 2018).

Generally, as NBR1 was shown to target HC-Pro for degradation (Hafrén, et al., 2018), this would lead to a loop of downregulation, with (1) NBR1-specific vasiRNA downregulating NBR1, (2) NBR1 degrading HC-Pro, and (3) HC-Pro suppressing the vasiRNA effect. Curiously, as I have shown, this nonetheless does not prevent NBR1 transcript and protein levels to increase upon TuMV infection.

The results of the studies by Li et al. (2020), which described decreased TuMV RNA accumulation in *Atnbr1*, and Hafrén et al. (2018) (more TuMV RNA accumulation in *Atnbr1*) contradict each other, making it

independent experiment. The complex interplay and interaction between induction of host gene expression by virus infection, their eventual silencing by vasiRNAs, and the suppression of the silencing by VSRs makes it hard to pinpoint a certain effect to a specific cause.

## 5.6) How does RDR1 mediate antiviral effects from a distance?

In the RDR1 transcriptional reporter experiment I showed that the RDR1 promoter sequence (which also includes the sequence downstream of RDR1) does not drive expression in the SAM but in and around the vasculature and below the meristem dome. Therefore, as RDR1 mitigates antiviral effects in the top layers of the SAM, some factors must move from the RDR1-expressing tissue into the meristem to achieve TuMV exclusion. Generally, there exist different possibilities: (1) that RDR1-dependent siRNAs move, (2) that the dsRNA product of RDR1 prior to dicing moves, or (3) that the RDR1 protein moves. As siRNAs are known to move throughout the plant, it is likely that they are the mobile molecules that mediate TuMV meristem exclusion (Melnik et al., 2011). Further experiments must be performed to investigate these possibilities. To see whether RDR1 itself is moving, immunolocalization or fluorescent tagging of RDR1 would be insightful experiments. Furthermore, to check for movement of siRNAs derived from RDR1, one could express artificial siRNA under the RDR1 promoter. By *in situ* staining with a complementary LNA probe, the location and distribution of the siRNA could be determined.

Additionally, single cell transcriptomics and sRNA-sequencing of mock- and TuMV-infected meristematic and inflorescence cells should prove to be valuable tools to unravel the underlying mechanics of the phenomenon.

## 6) References

- Alazem, M., Kim, K.-H., & Lin, N.-S. (2019). *Effects of Abscisic Acid and Salicylic Acid on Gene Expression in the Antiviral RNA Silencing Pathway in Arabidopsis*. *International Journal of Molecular Sciences*, 20(10), 2538. <https://doi.org/10.3390/ijms20102538>
- Amari, K., Boutant, E., Hofmann, C., Schmitt-Keichinger, C., Fernandez-Calvino, L., Didier, P., Ritzenthaler, C. (2010). *A family of plasmodesmal proteins with receptor-like properties for plant viral movement proteins*. *PLoS Pathogens* 6(9), e1001119. <https://doi.org/10.1371/journal.ppat.1001119>
- Bayer, E., Thomas, C., & Maule, A. (2008). *Symplastic domains in the Arabidopsis shoot apical meristem correlate with PDLP1 expression patterns*. *Plant Signaling & Behavior*, 3(10), 853–855. <https://doi.org/10.4161/psb.3.10.6020>
- Bond, D. M., & Baulcombe, D. C. (2014). *Genetic transitions leading to heritable, RNA-mediated de novo silencing in Arabidopsis thaliana*. *PNAS*, 112(3), 917–922. <https://doi.org/10.1073/pnas.1413053112>
- Bradamante, G., Incarbone, M., & Mittelsten-Scheid, O. (2021). *Under siege: virus control in plant meristems and progeny*. *Plant Cell*, 33(8), 2523–2537. <https://doi.org/10.1093/plcell/koab140>
- Burian, A. (2021). *Does Shoot Apical Meristem Function as the Germline in Safeguarding Against Excess of Mutations?* *Frontiers in Plant Science*, 12, 707740. <https://doi.org/10.3389/fpls.2021.707740>
- Cao, M., Du, P., Wang, X., Yu, Y.-Q., Qiu, Y.-H., Wanxiang Li, A. G.-O., Ding, S.-W. (2014). *Virus infection triggers widespread silencing of host genes by a distinct class of endogenous siRNAs in Arabidopsis*. *Proceedings of the National Academy of Sciences of the United States of America*, 111(40), 14613–14618. <https://doi.org/10.1073/pnas.1407131111>
- Carbonell, A. (2017). *Plant ARGONAUTES: Features, Functions, and Unknowns*. *Methodes in molecular biology* 1640, 1–21. [https://doi.org/10.1007/978-1-4939-7165-7\\_1](https://doi.org/10.1007/978-1-4939-7165-7_1)
- Charles, W. M., Attila, M., & Baulcombe, D. C. (2011). *Intercellular and systemic movement of RNA silencing signals*. *EMBO Journal*, 30(17), 3553–3563. <https://doi.org/10.1038/emboj.2011.274>
- Cuesta, R., Yuste-Calvo, C., Gil-Cartón, D., Sánchez, F., Ponz, F., & Valle, M. (2019). *Structure of Turnip mosaic virus and its viral-like particles*. *Sci Rep*, 9(1), 15396. <https://doi.org/10.1038/s41598-019-51823-4>
- Deleris, A., Gallego-Bartolome, J. G., Bao, J., Kasschau, K. D., Carrington, J. C., O., V. (2006). *Hierarchical Action and Inhibition of Plant Dicer-Like Proteins in Antiviral Defense*. *Science*, 313(5783), 68–71. <https://doi.org/10.1126/science.1128214>
- Di Serio, F., Martínez de Alba, A.-E., Navarro, B., Gisela, A., Flores, R. (2010). *RNA-dependent RNA polymerase 6 delays accumulation and precludes meristem invasion of a viroid that replicates in the nucleus*. *Journal of Virology*, 84(5), 2477–2489. <https://doi.org/10.1128/JVI.02336-09>

- Schwarz, D. S., Hutvagner, G., Du, T., Xu, Z., Aronin, N., & Zamore, P. D. (2003). *Asymmetry in the Assembly of the RNAi Enzyme Complex*. *Cell*, 115(2), 199–208. [https://doi.org/10.1016/s0092-8674\(03\)00759-1](https://doi.org/10.1016/s0092-8674(03)00759-1)
- Dodsworth S. (2009). *A diverse and intricate signalling network regulates stem cell fate in the shoot apical meristem*. *Developmental biology*, 336(1), 1–9. <https://doi.org/10.1016/j.ydbio.2009.09.031>
- Drinnenberg, I. A., Weinberg, D. E., Xie, K. T., Mower, J. P., Wolfe, K. H., Fink, G. R., & Bartel, D. P. (2009). *RNAi in budding yeast*. *Science*, 326(5952), 544–550. <https://doi.org/10.1126/science.1176945>
- Endres, M. W., Gregory, B. D., Gao, Z., Foreman, A. W., Mlotshwa, S., Ge, X., Pruss, G. J., Ecker, J. R., Bowman, L. H., & Vance, V. (2010). *Two plant viral suppressors of silencing require the ethylene-inducible host transcription factor RAV2 to block RNA silencing*. *PLoS pathogens*, 6(1), e1000729. <https://doi.org/10.1371/journal.ppat.1000729>
- Li, F., Zhang, C., Tang, Z., Zhang, L., Dai, Z., Lyu, S., Li, Y., Hou, X., Bernards, M., Wang, A. (2020). *A plant RNA virus activates selective autophagy in a UPR-dependent manner to promote virus infection*. *New Phytologist*, 228(2), 622–639. <https://doi.org/10.1111/nph.16716>
- Fernández-Calvino, L., Martínez-Priego, L., Szabo, Z., Guzmán-Benito, I., González, I., Canto, T., Llave, C. (2016). *Tobacco rattle virus 16K silencing suppressor binds ARGONAUTE 4 and inhibits formation of RNA silencing complexes*. *The Journal of general Virology*, 97(1), 246–257. <https://doi.org/10.1099/jgv.0.000323>
- Fletscher, J. (2018). *The CLV-WUS Stem Cell Signaling Pathway: A Roadmap to Crop Yield Optimization*. *Plants*, 7(4), 87. <https://doi.org/10.3390/plants7040087>
- Garcia-Ruiz, H., Takeda, A., Chapman, E. J., Sullivan, C. M., Fahlgren, N., Brempelis, K. J., Carrington, C. J. (2010). *Arabidopsis RNA-Dependent RNA Polymerases and Dicer-Like Proteins in Antiviral Defense and Small Interfering RNA Biogenesis during Turnip Mosaic Virus Infection*. *The Plant Cell*, 22(2), 481–496. <https://doi.org/10.1105/tpc.109.073056>
- Grangeon, R., Cotton, S., Laliberté, J.-F. (2010). *A model for the biogenesis of turnip mosaic virus replication factories*. *Communicative & Integrative Biology*, 3(4), 363–365. <https://doi.org/10.4161/cib.3.4.11968>
- Guo, Z., Li, Y., Ding, S.-W. (2018). *Small RNA-based antimicrobial immunity*. *Nature Reviews Immunology*, 19(1), 31–44. <https://doi.org/10.1038/s41577-018-0071-x>
- Hafrén, A., Üstün, S., Hochmuth, A., Svenning, S., Johansen, T., Hofius, D. (2018). *Turnip Mosaic Virus Counteracts Selective Autophagy of the Viral Silencing Suppressor HCpro*. *Plant Physiology*, 176(1), 649–662. <https://doi.org/10.1104/pp.17.01198>
- Hernandez-Lagana, E., Mosca, G., Mendocilla-Sato, E., Pires, N., Frey, A., Giraldo-Fonseca, A., Autran, D. (2021). *Organ geometry channels reproductive cell fate in the Arabidopsis ovule primordium*. *eLife*, 10, e66031. <https://doi.org/10.7554/eLife.66031>
- Incarbone, M., & Dunoyer, P. (2013). *RNA silencing and its suppression: novel insights from in planta analyses*. *Trends in Plant Science*, 18(7), 382–392. <https://doi.org/10.1016/j.tplants.2013.04.001>

- Jiang, J., Patarroyo, C., Cabanillas, D. G., Zheng, H., Jean-François, L. (2015). *The Vesicle-Forming 6K2 Protein of Turnip Mosaic Virus Interacts with the COPII Coatomer Sec24a for Viral Systemic Infection*. *Journal of Virology*, 89(13), 6695–6710. <https://doi.org/10.1128/JVI.00503-15>
- Johanse, E., Edwards, M. C., Hampton, R. O. (1994). *SEED TRANSMISSION OF VIRUSES: Current Perspectives*. *Annual Review of Phytopathology*, 32, 363–386. <https://doi.org/10.1146/annurev.py.32.090194.002051>
- Jones, A. L., Thomas, C. L., Maule, A. J. (1998). *De novo methylation and co-suppression induced by cytoplasmically replicating plant RNA virus*. *The EMBO Journal*, 17(21), 6385–6393. <https://doi.org/10.1093/emboj/17.21.6385>
- Kasschau, K. D., Xie, Z., Allen, E., Llave, C., Chapman, E. J., Krizan, K. A., Carrington, J. C. (2003). *P1/HC-Pro, a viral suppressor of RNA silencing, interferes with Arabidopsis development and miRNA uncton*. *Developmental Cell*. 4(2), 205–217. [https://doi.org/10.1016/s1534-5807\(03\)00025-x](https://doi.org/10.1016/s1534-5807(03)00025-x)
- Lee, W.-S., Fu, S.-F., Li, Z., Murphy, A. M., Dobson, E. A., Garland, L. G., Carr, J. P. (2016). *Salicylic acid treatment and expression of an RNA-dependent RNA polymerase 1 transgene inhibit lethal symptoms and meristem invasion during tobacco mosaic virus infection in Nicotiana benthamiana*. *BMC Plant Biology*, 16, 15. <https://doi.org/10.1186/s12870-016-0705-8>
- Leonetti, P., Ghasemzadeh, A., Consiglio, A., Gursinsky, T., Behrens, S.-E., Pantaleo, V. (2020). *Endogenous activated small interfering RNAs in virus-infected Brassicaceae crops show a common host gene-silencing pattern affecting photosynthesis and stress response*. *New Phytologist*, 229(3), 1650–1664. <https://doi.org/10.1111/nph.16932>
- Lewsey, M., Surette, M., Robertson, F. C., Ziebell, H., Choi, S. H., Ryu, K. H., Carr, J. P. (2009). *The role of the Cucumber mosaic virus 2b protein in viral movement and symptom induction*. *Molecular Plant-Microbe Interactions*, 22(6), 642–654. <https://doi.org/10.1094/MPMI-22-6-0642>
- Li, Y., Xiong, R., Bernardis, M., Wang, A. (2016). *Recruitment of Arabidopsis RNA Helicase AtRH9 to the Viral Replication Complex by Viral Replicase to Promote Turnip Mosaic Virus Replication*. *Scientific Reports*, 6, 30297. <https://doi.org/10.1038/srep30297>
- Liu, Q., Feng, Y., Zhu, Z. (2009). *Dicer-like (DCL) proteins in plants*. *Functional & Integrative Genomics*, 9(3), 277–286. <https://doi.org/10.1007/s10142-009-0111-5>
- López-Moya, J. J., García, J. A. (2008). *Potyvirus*. *Encyclopedia of Virology*, 3, 313–322. <https://doi.org/10.1016/B978-012374410-4.00475-1>
- Malhan, D., Bhatia, S., Yadav, R. K. (2015). *Genome wide gene expression analyses of Arabidopsis shoot stem cell niche cell populations*. *Plant Signaling & Behavior*, 10(4), e1011937. <https://doi.org/10.1080/15592324.2015.1011937>
- Melnyk, C. W., Molnar, A., Baulcombe, D. C. (2011). *Intercellular and systemic movement of RNA silencing signals*. *EMBO Journal*, 30(17), 3553–3563. <https://doi.org/10.1038/emboj.2011.274>
- Mourrain, P., Béclin, C., Elmayan, T., Feuerbach, F., Godon, C., Morel, J.-B., Vaucheret, H. (2000). *Arabidopsis SGS2 and SGS3 Genes Are Required for*

- Posttranscriptional Gene Silencing and Natural Virus Resistance*. Cell, 101(5), 533–542. [https://doi.org/10.1016/s0092-8674\(00\)80863-6](https://doi.org/10.1016/s0092-8674(00)80863-6)
- Muhammad, T., Zhang, F., Zhang, Y., Liang, Y. (2019). *RNA Interference: A Natural Immune System of Plants to Counteract Biotic Stressors*. Cells, 8(1), 38. <https://doi.org/10.3390/cells8010038>
- Müller, R. (2007). *Zur Rolle der Signaltransduktion in der meristematischen Entwicklung von Arabidopsis thaliana*. Heinrich-Heine-Universität Düsseldorf.
- Peele, C., Jordan, C. V., Muangsan, N., Turnage, M., Egelkrout, E., Eagle, P. R., Hanley-Bowdoin, L. (2001). *Silencing of a meristematic gene using geminivirus-derived vectors*. Plant Journal, 27(4), 357–366. <https://doi.org/10.1046/j.1365-313x.2001.01080.x>
- Pitzalis, N., Heinlein, M. (2018). *The roles of membranes and associated cytoskeleton in plant virus replication and cell-to-cell movement*. Journal of Experimental Botany, 69(1), 117–132. <https://doi.org/10.1093/jxb/erx334>
- Pitzalis, N., Amari, K., Graindorge, S., Pflieger, D., Donaire, L., Wassenegger, M., Heinlein, M. (2020). *Turnip mosaic virus in oilseed rape activates networks of sRNA-mediated interactions between viral and host genomes*. Communications Biology, 3(1), 702. <https://doi.org/10.1038/s42003-020-01425-y>
- Poque, S., Wu, H.-W., Huang, C.-H., Cheng, H.-W., Hu, W.-C., Yang, J.-Y., Yeh, S.-D. (2017). *Potyviral Gene-Silencing Suppressor HCpro interacts with Salicylic Acid (SA) binding Protein 3 to weaken the SA-mediated Defense Response*. Molecular Plant-Microbe Interactions, 31(1), 86–100. <https://doi.org/10.1094/MPMI-06-17-0128-FI>
- Qu, F., Ye, X., Hou, G., Sato, S., Clemente, T. E., Morris, T. J. (2005). *RDR6 has a broad-spectrum but temperature-dependent antiviral defense role in Nicotiana benthamiana*. Journal of Virology, 79(24), 15209–15217. <https://doi.org/10.1128/JVI.79.24.15209-15217.2005>
- Ruiz, M. T., Voinnet, O., Baulcombe, D. C. (1998). *Initiation and Maintenance of Virus-Induced Gene Silencing*. Plant Cell, 10(6), 937–946. <https://doi.org/10.1105/tpc.10.6.937>
- Scholthof, K.-B. G., Adkins, S., Czosnek, H., Palukaitis, P., Jacquot, E., Hohn, T., Foster, G. D. (2011). *Top 10 plant viruses in molecular plant pathology*. Molecular Plant Pathology, 12(9), 938–954. <https://doi.org/10.1111/j.1364-3703.2011.00752.x>
- Schwach, F., Vaistij, F. E., Jones, L., Baulcombe, D. C. (2005). *An RNA-Dependent RNA Polymerase Prevents Meristem Invasion by Potato Virus X and Is Required for the Activity But Not the Production of a Systemic Silencing Signal*. Plant Physiology, 138(4), 1842–1852. <https://doi.org/10.1104/pp.105.063537>
- Shabalina, S. A., Koonin, E. V. (2008). *Origins and evolution of eukaryotic RNA interference*. Trends Ecology Evolution, 23(10), 578–587. <https://doi.org/10.1016/j.tree.2008.06.005>
- Shu, Q. Y., Forster, B. P., Nakagawa, H. (2012). *Plant Mutation Breeding and Biotechnology*. Food and Agriculture Organization of the United Nations (FAO) and International Atomic Energy Agency (IAEA).

- Takahashi, H., Fukuhara, T., Kitazawa, H., Kormelink, R. (2019). *Virus Latency and the Impact on Plants*. *Frontiers in Microbiology*, 10, 2764. <https://doi.org/10.3389/fmicb.2019.02764>
- Tang, L. P., Li, X. M., Dong, Y. X., Zhang, X. S., Su, Y. H. (2017). *Microfilament Depolymerization Is a Pre-requisite for Stem Cell Formation During In vitro Shoot Regeneration in Arabidopsis*. *Plant Science*, 8, 158. <https://doi.org/10.3389/fpls.2017.00158>
- UniProt. (2021). *POLG\_TUMVQ*.
- Valli, A. A., Gallo, A., Rodamilans, B., López-Moya, J. J., García, J. A. (2018). *The HCPro from the Potyviridae family: an enviable multitasking Helper Component that every virus would like to have*. *Molecular Plant Pathology*, 19(3), 744–763. <https://doi.org/10.1111/mpp.12553>
- Vijayapalani, P., Maeshima, M., Nagasaki-Takekuchi, N., Miller, W. A. (2012). *Interaction of the Trans-Frame Potyvirus Protein P3N-PIPO with Host Protein PCaP1 Facilitates Potyvirus Movement*. *PLoS Pathogens*, 8(4), e1002639. <https://doi.org/10.1371/journal.ppat.1002639>
- Viralzone. (2012). SIB Swiss Institute of Bioinformatics.
- Voinnet, O., Vain, P., Angell, S., Baulcombe, D. C. (1998). *Systemic Spread of Sequence-Specific Transgene RNA Degradation in Plants Is Initiated by Localized Introduction of Ectopic Promoterless DNA*. *Cell*, 166(3), 779. <https://doi.org/10.1016/j.cell.2016.07.014>
- Wang, X.-B., Wu, Q., Ito, T., Cillo, F., Li, W.-X., Chen, X., Ding, S.-W. (2010). *RNAi-mediated viral immunity requires amplification of virus-derived siRNAs in Arabidopsis thaliana*. *Proceedings of the National Academy of Science of the United States of America*, 107(1), 484–489. <https://doi.org/10.1073/pnas.0904086107>
- Willmann, M. R., Endres, M. W., Cook, R. T., Gregory, B. D. (2011). *The Functions of RNA-Dependent RNA Polymerases in Arabidopsis*. *The Arabidopsis Book*, 9, e0146. <https://doi.org/10.1199/tab.0146>
- Wu, H., Qu, X., Dong, Z., Luo, L., Shao, C., Forner, J., Zhao, Z. (2020). *WUSCHEL triggers innate antiviral immunity in plant stem cells*. *Science*, 370(6513), 227–231. <https://doi.org/10.1126/science.abb7360>
- Xu, T., Zhang, L., Zhen, J., Fan, Y. (2013). *Expressional and regulatory characterization of Arabidopsis*. *Planta*, 237(6), 1561–1569. <https://doi.org/10.1007/s00425-013-1863-7>
- Ying, X.-B., Dong, L., Zhu, H., Duan, C.-G., Du, Q.-S., Lv, D.-Q., Guo, H.-S. (2010). *RNA-Dependent RNA Polymerase 1 from Nicotiana tabacum Suppresses RNA Silencing and Enhances Viral Infection in Nicotiana benthamiana*. *Plant Cell*, 22(4), 1358–1372. <https://doi.org/10.1105/tpc.109.072058>
- You, C., He, W., Hang, R., Zhang, C., Cao, X., Guo, H., Mo, B. (2019). *FIERY1 promotes microRNA accumulation by suppressing rRNA-derived small interfering RNAs in Arabidopsis*. *Nature Communications*, 10(1), 4424. <https://doi.org/10.1038/s41467-019-12379-z>

Zavaliev, R., Ueki, S. L. Epel, B. (2010). *Biology of callose ( $\beta$ -1,3-glucan) turnover at plasmodesmata*, Protoplasma, 248(1), 117–130. <https://doi.org/10.1007/s00709-010-0247-0>

## 7) Annex

### 7.1) Solutions and buffers

#### Virus inoculation buffer

Sodium phosphate pH 7.2	50 mM
Sodium Sulfite	0,2% (w/v)

#### Fixing solution

2x MTSB	4ml
Triton	0,1% (w/v)
Formaldehyde	2% (w/v)
ddH <sub>2</sub> O	ad. 8 ml

#### ClearSee®

Xylitol powder	10% (w/v)
Sodium deoxycholate	15% (w/v)
Urea	25% (w/v)
(DAPI)	0,2% (w/v)

#### 2x MTSB solution

PIPES	7,5 g
EGTA	0,95 g
MgSO <sub>4</sub> ·7H <sub>2</sub> O	0,61 g
KOH	1,25 g
ddH <sub>2</sub> O	ad. 250 ml

#### Tris-Glycine buffer 10x

Tris	60,4 g
Glycine	288 g
ddH <sub>2</sub> O	ad. 2 L

#### DNA extraction buffer

Tris-HCl	50mM
NaCl	300mM
Sucrose	300mM
pH =	7,5

#### Laemmli buffer 2x

SDS	4%
Beta-mercaptoethanol	10%
Glycerol	20%
Tris	0,1%
Bromophenol blue	0,005%
pH =	6,8

## 7.2) List of Abbreviations

Abbreviation	Meaning
AGO	argonaute protein
CaMV	<i>Cauliflower mosaic virus</i>
CMV	<i>Cucumber mosaic virus</i>
CymRSV	<i>Cymbidium ringspot virus</i>
DCL	dicer-like protein
dpi	days post infection
dsRNA	double stranded RNA
L1	Meristematic dome cell layer 1
L2	Meristematic dome cell layer 2
L3	meristematic dome cell layer 3
OC	organizing center
PDLP1	plasmodesmata located protein 1
PPFD	photosynthetically active photon flux density
PSbMV	<i>Pea seed-borne mosaic virus</i>
PSTVd	<i>Potato spindle tuber viroid</i>
PVX	<i>Potato virus X</i>
PVY	<i>Potato virus Y</i>
RDR	RNA-dependent RNA polymerase
RI	refractive index
RISC	RNA-induced silencing complex
RNAi	RNA interference
SAM	shoot apical meristem
siRNA	small interfering RNA
TGMV	<i>Tomato golden mosaic virus</i>
TRV	<i>Tobacco rattle virus</i>
TuMV	<i>Turnip mosaic virus</i>
TVCV	<i>Turnip vein-clearing virus</i>
vasiRNA	virus-activated small interfering RNA
VIGS	virus-induced gene silencing
vsRNA	virus-derived small interfering RNA
VSR	viral suppressors of RNA silencing
WT	wild type
WUS	WUSCHEL